Progress in Aerospace Sciences 50 (2012) 1–26

Contents lists available at SciVerse ScienceDirect

Progress in Aerospace Sciences

journal homepage: www.elsevier.com/locate/paerosci

The flow field in turbulent round free jets

C.G. Ball [a], H. Fellouah [b], A. Pollard [c,*]

[a] Graduate School of Medicine, University of Wollongong, Wollongong, New South Wales, Australia
[b] Département de génie mécanique, Université de Sherbrooke, Sherbrooke, Québec, Canada
[c] Department of Mechanical and Materials Engineering, Queen's University, Kingston, Ontario, Canada

ARTICLE INFO

Available online 8 February 2012

Keywords:
Characterisation
Initial conditions
Similarity
Length scales
Spectral analysis
Coherent structures

ABSTRACT

A critical review of both experimental and computational studies of round turbulent jets is provided, beginning with the work of Tollmien (1926). This review traces the history, the major advances, and the various stages that the research community went through over the past 85-odd years—from statistical analyses through to the use of conditional sampling, proper orthogonal decomposition and structural eduction methods. It includes the introduction of novel experimental techniques as well as insights gained from recent large eddy and direct numerical simulations. Some direction where future research may prove beneficial is also provided.

The review does not include the effects of passive or active control, scalar contaminant transport whether by heat or mass. It includes effects of Reynolds number, inlet conditions (excluding swirl) and considers both near- and far-field investigations. We have minimised reference to papers that utilise models of turbulence unless such works provide something of particular importance.

Contents

1. Introduction

The study of turbulent flow has evolved over the last century from a curiosity to an intensely explored research theme. During this period, the physical insight that we have gained has developed alongside the evolution of theoretical, experimental, and computational methods. In the broadest view, progression in turbulence research may be seen as periodic. Numerous research groups around the world have emerged as 'schools' in turbulence during developmental periods built upon then-current ideas; these schools were built around statistical, experimental, computational, and other methods.

Here is a **very** brief description of idealogical paradigms and the inception of their associated schools. The basic ideas of Reynolds and Prandtl gave rise to a school of statistical turbulence that laid the

* Corresponding author.
E-mail address: pollard@me.queensu.ca (A. Pollard).
URL: http://me.queensu.ca/people/pollard (A. Pollard).

0376-0421/$ - see front matter © 2011 Elsevier Ltd. All rights reserved.
doi:10.1016/j.paerosci.2011.10.002

groundwork for computational turbulence and its schools on both modelling and simulation. Experimental turbulence research began with simple Pitot tubes, followed by hot-wire anemometry and today's advanced laser-based methods that are fast approaching the fidelity in space and time that is currently solely the purview of direct numerical and large eddy simulation (DNS, LES). From the application of these techniques and technologies the bewildering array of length and time scales, embodied as we now know within turbulence and its structure, has emerged to challenge the turbulence community to control turbulence rather than to merely design and build devices that are subject to the 'whims' of a flow.

Canonical turbulent flows include boundary layers, channel flows, the wake, jets, and others. Each of these has an extensive literature which appears to grow ever more as we direct ever improving tools and techniques toward, according to Richard Feynman 'the last great unsolved problem in classical physics.' In this paper, we review the 'simple' free round turbulent jet that carries no additional thermo-physico-chemical effects (such as density variation, heat release, et cetera) and that operates in the absence of any geometric modifications to the nozzle (such as lobes, for example). Nozzle effects are considered only insofar as their use to illuminate flow physics and improve our understanding of flows.

2. The round jet: from birth to death

The jet is borne out of the nozzle exit plane. As the jet issues into a quiescent environment, as supposed here for this review, it will eventually entrain the receiving fluid and spread in the radial direction with downstream distance until the initial momentum is spread very thinly to the point where viscous action will dissipate energy and lead to the 'death' of the jet.

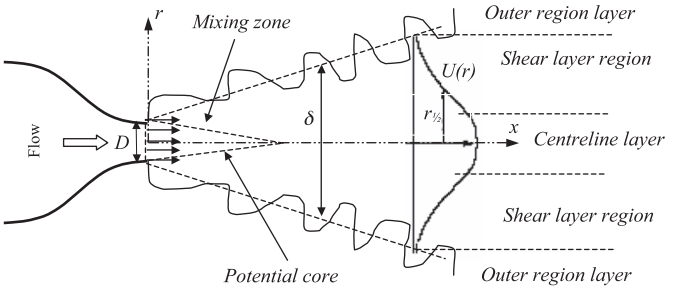

Fig. 1. Schematic of a free jet issuing from a smooth-contraction nozzle and its co-ordinate system.

Even though downstream development of jets depends on both initial and boundary conditions, it is possible to define a generic co-ordinate system that can be applied to the majority of jet flows. The flow field geometry of a jet issuing from a smooth nozzle is shown in Fig. 1. A polar co-ordinate system is used, as shown, with the x-direction aligned with the nozzle axis. The velocity components in the x, r, and θ co-ordinate directions are denoted U, V, and W, respectively. The terms in the Reynolds decomposition are herein denoted $u=U+u'$, $v=V+v'$, and $w=W+w'$. From the nozzle with outlet diameter D flows a Newtonian fluid with characteristic velocity U_j. The centreline velocity is U_c. A commonly used characteristic length, the jet half-radius $r_{1/2}$ is determined by $U_{r_{1/2}}=U_c/2$. The local time-averaged diameter of the jet is denoted δ and is referred to as the outer scale. All data gathered from the literature are herein referred to in this manner.

In Fig. 1, the convoluted edge represents the shear layer between the high vorticity jet flow and the nearly-at-rest surrounding fluid [1]. As air from the irrotational ambient fluid is entrained, the mass flux of the jet increases with axial position x; momentum flux, however, remains, as it must, constant.

Different axial regions are defined in the axisymmetric round jet: the near field, the intermediate field, and the far field. The near field, defined by its potential core which appears only for jets issuing from a contraction nozzle, is a region of flow establishment; its flow features meet those of the surrounding mixing zone and cause the development of turbulence; it is usually within $0 \le x/D \le 7$.

The initial instability modes, created by the jet at its source, produce the flow structures in the shear layer (or mixing zone); the resultant vortices will roll-up and then pair-up, as depicted in Fig. 2. The intensity of vortex pairing depends on initial conditions (being much weaker or non-existent in pipe jets, for example). The mean velocity profile at the exit is determined by its geometry; a nozzle, pipe, or sharp-edged orifice will each produce a top-hat, power-law-type, or complex converging-diverging flow profile, respectively. Historically, as is discussed later, the flow characteristics created by these profiles were believed to be washed away as the flow evolves downstream into the far field;

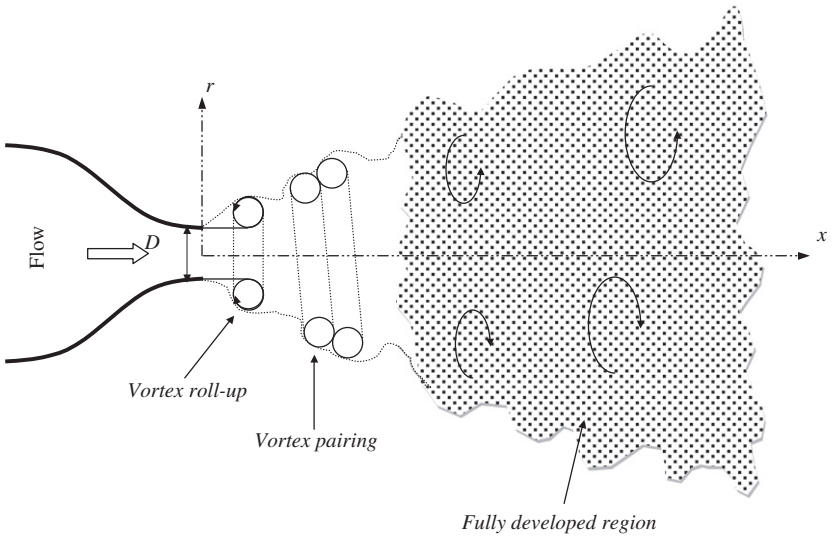

Fig. 2. Flow features of the free round jet.

it is now known that initial conditions have a direct impact on the entire flow.

The far field, located from approximately $x/D \geq 70$ [2, Chapter 2], is the fully-developed or self-similar region where, with appropriate scaling, the thin shear layer approximations (where axial gradients are assumed to be much smaller than radial gradients) hold. Here, the flow is self-preserving and is considered to be in equilibrium; this is one reason, among many possible, that this region has been the subject of considerable research. The terms 'self-similar' and especially 'equilibrium,' in this case, are loosely defined. In Kolmogorov's Universal Equilibrium Theory it is offered that small scale eddies are locally isotropic and in approximate statistical equilibrium with the large scale eddies [3]. Whereas George [4] (see also, for example, Johansson et al. [5]) argues that equilibrium similarity requires that 'the terms of the governing equations must maintain the same relative balance as the flow evolves.' This is the region where the fine scales of turbulence can be usefully interrogated (a strong incitement for research); see, for example, Sreenivasan and Antonia [6] and the references therein.

The transition region between the near and far fields (within $7 \leq x/D \leq 70$) is, in our opinion, the most intriguing but least studied region of the round free turbulent jet. It is within this region of the flow where the highly anisotropic turbulent structures, formed within the first few diameters of the nozzle, evolve and interact; this, as will be noted, is Reynolds number dependent. The near to intermediate field (NIF, $0 \leq x/D \leq 30$) often dominates practical applications of a jet for which upstream conditions can significantly influence heat, mass, and momentum transfer. Therefore, the ability to control the flow development in the NIF would have a vital impact on many engineering applications, such as jet noise and mixing. A jet must be receptive to external influences before its natural evolution can be modified. Current examples of this are described in Samimy et al. [7], Mitsuishi et al. [8], Wei and Freund [9], and Hall et al. [10].

In the radial direction, three concentric layers are readily identified, as shown in Fig. 1. These are the centreline region, the shear layer, and the outer layer. In the centreline region, the flow's maximum axial mean velocity is found on the centreline; here, turbulence evolves with axial position to eventually reach equilibrium and far-field characteristics. In the shear layer, the radial velocity gradient causes vortex cores to form, evolve, and pair to create large eddies. There is evidence that these vortex cores are interlinked with axial (or longitudinal) vorticity to create structures referred to as 'braids' (these are addressed later in this review). The large eddies break down and form smaller and smaller eddies; that is, the turbulence structures diminish in scale in both time and space. Throughout this process, energy is transferred from the large scale structures to the smaller. Velocities in the outer layer, typically of order $U_c/10$, rapidly fall to the free stream value as $r \to \infty$. With this, we are reminded of Richardson's suggestion that

> Big whirls have little whirls,
> that feed on their velocity;
> and little whirls have lesser whirls,
> and so on to viscosity [11].

We now survey, in detail, the free round turbulent jet.

3. The two jet ages

While it is uncertain whether one led to the other, it is interesting that the beginnings of research into the round jet paralleled the dawn of the jet age in aviation. The beginnings of both jet ages, aviation and turbulent, are outlined here.

In popular culture, the aviation jet age may be considered to have begun with the first scheduled flight of the passenger jet airliner, the de Havilland Comet, in 1952. However, the jet engine saw its birth in the 1920s and 1930s. After writing his graduation thesis in 1928, registering the first patent for the jet engine in 1930, and founding a company in 1936, Sir Frank Whittle successfully teamed with A.A. Griffith (of the Royal Aircraft Establishment) and Henry Tizard (then rector of Imperial College London and chairman of the Aeronautical Research Committee) to operate the first jet engine, the 'Whittle Unit (WU),' on April 12, 1937. A variant of this engine powered the first jet aircraft flight in the United Kingdom on May 15, 1941. The Whittle Supercharger Type W.1 powered the Gloster E.28/39, flown by Flight Lieutenant P.E. Gerry Sayer, that took off from RAF Cranwell, U.K. at 19:40 May 15, 1941 to fly for nearly 20 min and reach speeds of 545 km/h. (The Whittle Laboratory at Cambridge University opened in 1973.)

Meanwhile, Hans Joachim Pabst von Ohain independently undertook similar tasks in Germany. In 1933, von Ohain formulated his theory of jet propulsion; in 1935 he earned his Ph.D. in physics at the University of Göttingen. By September 1937, he had built a factory-tested demonstration jet engine. Ernst Heinkel then designed and constructed the Henkel He178 that, flown on August 27, 1939, by Flight Captain Erich Warsitz, would be the world's first jet powered aircraft flight.

With the dawn of the jet age, jet engines, and jet flight, came the inspiration for increased research and improved understanding of jets. It may well be that a surge of research into the canonical jet flow of fluid mechanics was concomitant with military, government and corporate interest in jet propulsion. Research into the fluid dynamics of jet flows progressed rapidly in those early years; emergent knowledge on jets is collected in *The Theory of Turbulent Jets* by Abramovich [12]. The first **experimental** investigations of a round jet were performed by Ruden [13] and Kuethe [14], according to Dowling and Dimotakis [15].

By 1944 it was boldly declared that 'the problem of the flow in a round jet, when the air surrounding the jet is at rest, has been fully investigated' [16]. Despite, or perhaps precipitating, this presumptuous statement, Squire and Trouncer [16] drew several very insightful conclusions – some of which have been 'rediscovered anew' over the years – into the nature and research of jet flows.

First, it was noted that the outer boundary of the jet is difficult to identify experimentally and is often actually wider than determined in calculations. Because of this, Squire and Trouncer [16] proposed that the 'half-velocity' (which we now know as $r_{1/2}$) should be a reliable indicator of jet width.

Second, a physical explanation of the mass flow in the jet was offered; this description is most interesting because it hints at the developments that later arose from the work of Wygnanski and Fiedler [17]—especially, an understanding of implications of the infinite space into which many actual experimental jets rigs are assumed to issue. The description is repeated here verbatim:

> The mass flow across each section of the jet can be calculated, and is found to increase more rapidly than the increase provided for by the natural inflow into the growing jet from the external stream: the jet thus induces an inflow towards itself. To do this, the pressure inside the jet must be lower than in the free stream and this appears to be in contradiction to the previous assumption of uniform pressure; it has, however, been shown by Tollmien [18] that this reduction in pressure is extremely small for a jet issuing into a fluid at rest [16].

Perhaps most importantly, it was surmised by Squire and Trouncer [16] and later specifically affirmed by Ricou and Spalding [19] that the characteristic length of a turbulent jet should not

be the orifice diameter, D, but rather $D(\rho_0/\rho_1)^{1/2}$, where ρ_0 is the density of the jet fluid and ρ_1 is that of the surrounding fluid. The inclusion of fluid properties (density, in this case) acknowledges that the choice of working fluid may affect the flow, and it is a step toward a more relevant characteristic length. As will be shown herein, it has been proposed that a physically meaningful characteristic length should be used instead of a merely convenient jet diameter.

In the years before and after 1944, there were other significant developments in research in jet flows. Turbulent jet mixing of incompressible fluids issuing from a smooth contraction nozzle was considered theoretically by Tollmien [18] through Prandtl's mixing length theory. With the goal to extend Tollmien's results to other cases of practical importance, analytical and experimental studies of the plane jet and the round jet were described by Kuethe [20,14]. In this work, Kuethe confirmed that Tollmien's solution in which the round jet is considered to issue from a point source holds well for large x, far beyond the potential core. Additionally, the following description (likely one of the first such descriptions) was offered:

> A schematic longitudinal section of the flow is shown in Fig. 3. Region A consists of the annular mixing region surrounding the core of potential flow. In region B the entire jet is a mixing region and the central velocity u_0 decreases as x increases. The velocity profiles and the x gradient of u_0 finally reach an asymptotic state as the fluid enters the region C. In C, the central velocity is inversely proportional to the distance from some point near the jet mouth and all profiles are similar... It is in this last region that Tollmien's solution is valid [14].

Writing 'some point near the jet mouth,' Kuethe suggests the virtual origin.

Corrsin, in his reports to the National Advisory Committee for Aeronautics (NACA; including [21,22]), made significant early contributions and advances to research in jet flows. In 1943, he alluded to the problem of the definition of similarity in jet flows that we face still today [21]; Corrsin first confirmed the conclusions made separately by Ruden [13] and Kuethe [14], then added some thought and depth to the definition of similarity. He wrote:

> Ruden [13] and Kuethe [14] have both made measurements in jets with axisymmetry. Ruden measured velocity and temperature distributions out to an axial distance of about 15 diameters in a heated jet; while Kuethe measured detailed velocity distributions and made some turbulence measurements out to 9 diameters in an unheated jet. Both investigators found that similarity of velocity profiles was reached before 10 diameters, which led to the general belief that complete mechanical similarity in a jet was reached there. However, it was thought that the turbulence distribution in a radial direction might serve as an indication of a fully developed state. Furthermore, it was felt that the limit of 15 diameters, which appeared to be the greatest axial distance included in any previously published results, might be insufficient to give a comprehensive picture of the nature of the flow [21].

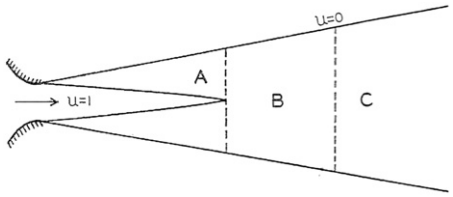

Fig. 3. Schematic section of the flow from a circular nozzle. Reprinted with permission, from [14]; ASME International. *N.B.: There is no scale associated with this figure*; *the fully developed region is not normally found until beyond* $x/D > 70$.

Even with the uncertainty of the detailed physical form of King's law equation for the heat loss from a fine wire to a moving fluid [23], the development of the hot-wire technique for the simultaneous measurement of temperature and velocity fluctuations made it possible to study turbulent heat transfer from the standpoint of both mean and fluctuating variables [24]. Corrsin obtained hot-wire measurements of flow from a round jet with a Reynolds number of 103,000 (produced with both a 1-in. and a 3-in. diameter nozzle) that were taken in the region from the end of the potential cone to an axial distance of $40D$ downstream. Among other notable conclusions from this study was the description of the flow as a core surrounded by two concentric annuli (the three concentric layers described in Section 2). Furthermore, beyond the potential core, a completely turbulent flow exists in the core region from the axis to (now termed) $r_{1/2}$. Outside of this core is a wide annular transition region; and, outside of the transition region to the edge of the jet, the flow is like a laminar collar. Corrsin also states that similarity of velocity and turbulence profiles is not attained until at least $x/D > 20$ where the turbulence profile of u'/U_c loses its local minimum on the axis [21]. For a half jet, the velocity field was carefully documented by Liepmann and Lauffer [25] who found that after 300 initial momentum thicknesses downstream of the trailing edge of the splitter plate, the velocity profiles could be expressed by a single velocity and length scale—in this condition, the flow can be called self-preserved.

Continuation of the work reported in Corrsin [21] was described several years later by Corrsin and Uberoi [22]. Perhaps most significantly, but not uniquely, it was proposed that a physically meaningful characteristic length should be used instead of the commonly used nozzle diameter. The text of that proposal is repeated here:

> Although [$r_{1/2}$] has been used as a characteristic jet width in most of the previous figures, it is clear that a width definition of greater physical significance can be made on the basis of momentum flow. The 'momentum diameter' of the jet at any section
>
> $$\Delta = 2\sqrt{2}\left(\int_0^\infty \frac{q}{q_{max}} r\, dr\right)^{1/2} \quad (1)$$
>
> [where $q \equiv$ dynamic pressure ($\frac{1}{2}\rho\overline{U}^2$) and $q_{max} \equiv$ maximum dynamics pressure at a section] is defined as the diameter of a jet of rectangular density and velocity profiles ($\rho = \rho_{min}$ and $\overline{U} = \overline{U}_{max}$), whose total rate of flow of axial momentum is the same as in the actual jet at that section. Since the momentum flow in a free jet is effectively constant, this characteristic diameter is particularly convenient. It is analogous to the momentum thickness of a boundary layer, except that the latter is based on the momentum defect [22].

The main features deduced from experimental and theoretical studies of steady flow of a jet issuing from a nozzle into the surrounding stream at rest were presented by Pai in his book titled *Fluid Dynamics of Jets* [26]. It is useful to note that the subject has advanced considerably in the intervening 50 or so years since this book was published; however, it does provide a good introduction to the theory of inviscid, laminar and turbulent jet flows. Additionally, the review of mixing and injection of fluid is nicely summarised to about 1979 by Schetz [27].

Up to this point, key studies into jet flows were relatively focussed—researchers sought to develop physical and analytical understanding, even with a largely incomplete picture of the jet flow. Experimental investigations and descriptions of the flows

were, in one way or another, not comprehensive; this is to be expected, the technology required to acquire such knowledge was (and still is) developing alongside the understanding of jet flows. Improved experimental measurements of the jet flow that were needed were provided by Laurence [28] who described hot-wire anemometry techniques alongside a thorough investigation and description of high Reynolds number subsonic jets. Measurements were presented of velocity profiles, turbulence intensities, autocorrelations, longitudinal and lateral correlations, and spectra of turbulence for jets with Mach numbers ranging from $0.2 \leq Ma \leq 0.7$ ($Re = 192{,}000$–$725{,}000$) for round jets up to a distance of about $20D$. In addition, he also provided longitudinal and lateral velocity correlations and the single-point autocorrelations in a fixed reference frame over the entire region of the jet (again, up to about $20D$). To place the novelty of his work in context, Laurence noted 'an autocorrelator using a magnetic tape recorder and a special playback instrument was used to measure the velocity correlations. These autocorrelations were converted to longitudinal correlations that agreed well with the directly measured longitudinal correlations' [28]. This NACA report is recommended reading to novice turbulence researchers.

As a result of this effort, Laurence reported four primary results; these were: (1) regarding the change in position (relative to the axis) of maximum turbulence intensity with downstream location, (2) regarding the independence of scales of turbulence with Mach and/or Reynolds number and their changing relationship with distance from the nozzle, (3) regarding 'correlograms' and spectra and their resultant scales, and (4) regarding autocorrelations (and their autocorrelator) [28].

The foundation discoveries of the first 30 years or so of jet research, including the meticulous experimental survey and use of technology demonstrated in Laurence [28], set a standard for jet flow research to which we still adhere today—even as we face similar research problems. The motivation for Laurence's investigations, noise, also drives substantial modern research—this is but one of many unsolved aspects of jet flows.

4. Discovery

Nowadays, we continue in the discovery that began in the late 1950s and early 1960s. While our investigative techniques mature to solve ever more sophisticated problems, we still follow the path set out by the leaders of 60 years ago—consider landmark papers such as that by Laurence [28], as well as those by Ricou and Spalding [19], and Wygnanski and Fiedler [17]. We also follow the lead set out in the origination of the Journal of Fluid Mechanics, founded in 1956 by George K. Batchelor who 'was careful to ensure that the first few volumes contained papers which appealed to relatively young people, so that the readership would grow into the journal' and 'that there was little or no support for the idea of a new journal in fluid mechanics in 1956 from people over 40' [29]. Those who were then under 40 had established or belonged to the various schools of research in fluid mechanics (examples include Marseille, Cambridge, Johns Hopkins) and from which emerged key approaches to solving the problem of turbulence. With many (or some) of those who were then under 40 being still active in turbulence (and jet flows) research, we now approach the end of a first generation of discovery in jet flows.

Like the global variation in discovery methods in turbulence, research in jet flows has seen multiple approaches and foci. In this 'modern' review of the turbulent round jet, we classify and present studies under the following categories: Characterisation (distributions of mean velocity, turbulence intensity, spectra, et cetera), Entrainment (and the spread rate of the jet); Length Scales; Initial Conditions and Similarity; Spectral Analysis; Coherent Structures; and finally a section to summarise, and to offer suggestions for future work.

For those who are interested, the archival literature contains many papers that address the near field of jets that issue from orifices that are either passively or actively manipulated through the introduction of tabs (e.g. Zhang and Schneider [30] and Waterman et al. [31]), or micro-electro-mechanical systems (e.g. Suzuki et al. [32]). Such topics are not covered here.

4.1. Characterisation

The need to align analytical predictions with physical reality provides impetus for 'simple' measurement and characterisation of the flow field from a round jet. The complexity of this task is revealed implicitly in this section. The challenges to obtain and then verify accurate measurements of convective properties is compounded by the many ways in which velocity (turbulence) can be interpreted. And so, we continue to build upon early 'basic' measurements. We still seek thorough veracious characterisation of the flow from a round jet.

After 1960, the jet was investigated by an increasing number of researchers. Davies et al. [33] used a single hot-wire anemometer to investigate the near field of a round free air jet for Mach numbers ranging from 0.2 to 0.55. With these turbulence measurements, it was demonstrated that there exists a well-defined similarity relationship for the first six or eight diameters of the jet flow (along with the already known similarity farther downstream). These relationships degenerate near the jet orifice where the shear layer is very thin. Kinematic similarity can be established for intensity, space scales, time scales, and spectra, all in terms of the distance from the jet orifice, and for a local time scale that is most suitably expressed in terms of the inverse of the local shear. It was found that the length scale is proportional to the distance from the jet orifice. However, the maximum shear is also related to this distance as well as to the jet efflux velocity.

The near field of the jet (over $1 \leq x/D \leq 10$ for $Re_D = 220{,}000$) was explored experimentally by Sami et al. [34] using both Pitot-static probes and hot-wire anemometers. In this study, it was observed that the root-mean-square pressure and Reynolds shear stress profiles were similar in the near field ($x/D < 10$). The results of intermittency measurements showed, in the flow establishment region, that mean-axial turbulence intensities in the jet are not uniform. The Taylor micro-scale was, furthermore, seen to be independent of the jet velocity and increased with distance from the outflow section.

One of the most influential papers on the round jet is that of Wygnanski and Fiedler [17]. In their extensive experimental work, they presented profiles for mean velocities, second and third order single-point correlations, energy balances, and length scales. Rodi [35] later applied a new method for analysis of hot-wire signals to measure mean velocity and turbulence intensity profiles. In a subsequent analysis of both sets of results, Seif [36] discovered significant momentum losses in the data of Wygnanski and Fiedler [17] that of course violate the conservation law. This is not to denigrate the paper by Wygnanski and Fiedler. In fact, the work unintentionally reinforced an important lesson when comparing computational to experimental data: compute using the **same** boundary conditions as in experiment!

As noted earlier, discussion of nozzle and inlet effects is not within the purview of this paper; adequate treatment would require (at least) a dedicated review. Interested readers are directed to the review by Nathan et al. [37]. An overview is unquestionably necessary because inlet conditions determine downstream conditions, flow development, and so forth—the topics of this paper.

In contrast to the classical treatment of Hinze [38], it is suggested by George in a theoretical analysis that turbulent jet flows can become asymptotic to a variety of self-similar states, as determined by their initial conditions [4,39]. There have been significant efforts to reconcile the classical hypothesis of universal similarity with the analytical result of George [4]. Some review articles on self-similarity of the scalar field provide inconsistent results. For example, the conclusions of Richards and Pitts [40] support the hypothesis of universal self-similarity of a jet flow; they concluded that the asymptotic state of the scalar field has little dependence on initial conditions; meanwhile, Dowling and Dimotakis [15] found a Reynolds number dependence of the far-field decay rate of the mean concentration field and the radial distribution of the r.m.s. concentration fluctuations. More recently, Mi et al. [41] examined the flow field for two jets (one with a contraction nozzle, the other with a long pipe inlet) over $0 \le x/D \le 70$ to verify the analytical results of George [4] and confirmed that the turbulent scalar properties throughout the jet flow are dependent on initial conditions. It was, again, re-affirmed that a universal asymptotic state of turbulence, independent of initial conditions, is unlikely to exist [41]. It is known that various nozzle shapes, as described in the archival literature and sketched here in Fig. 4, are used to generate different mean velocity profiles. A simple characterisation is that a contraction nozzle produces a top-hat velocity profile; a pipe nozzle produces a fully developed turbulent pipe flow profile, and a sharp-edged nozzle produces a saddle-backed profile (in this case, the hour-glass shaped interface between the jet and the free stream is known as the vena contracta effect [42]). Uddin and Pollard [43] showed that the jet initial conditions are important in the determination of the location of the virtual origin—the axial expansion of the effective jet width depends on the shape of the initial jet velocity profile. A thorough review of the effects of initial conditions (both steady and time-variant) on mixing in a jet is provided by Nathan et al. [37]. With regard to jets with steady inlet conditions, it is again concluded that jet inlet conditions (nozzle exit profiles) influence both the near- and far-field flows. The influence of initial conditions is attributed to the underlying structure of turbulent motions that is carried from the jet inlet throughout the flow field; the notion that alteration of initial conditions causes considerable modification of the large-scale vortices – especially in both their shape and convection velocities – has been confirmed independently [44,45]. According to Nathan et al. a jet never forgets [37].

The mechanism by which structures propagate downstream can be difficult to elucidate experimentally because of the expansive measurements that are required—in the far-field, one must collect many measurement points in a large three-dimensional space over a relatively long time-scale. Using volume-based measurements, Yoda et al. [46,47] compared the effects of nozzle oscillation on the downstream structures and modes of jets at three different Reynolds numbers (considering both papers, ranging from $Re_D = 1000$ to $Re_D = 5000$; well below the mixing transition, that is $Re < 20,000$, as will be discussed later). The authors report that both the natural and excited jets tend to oscillate in a pseudo-planar sinusoidal-like motion; this is explained as a superposition of simultaneous $+1$ and -1 helical modes. It was, furthermore, proposed that changes in pitch of the jet helix would likely result from differences in the jet exit flow [47].

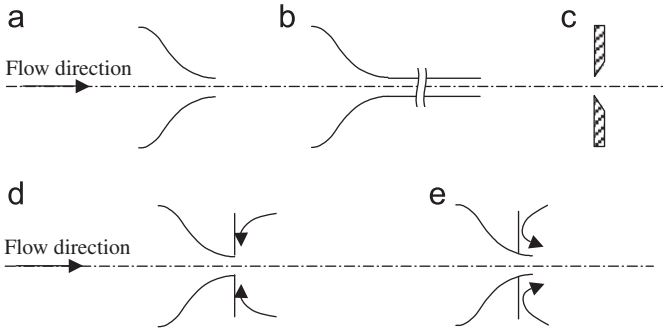

Fig. 4. Various nozzle shapes and initial boundary conditions. (a) Contraction, (b) pipe, (c) sharp-edged, (d) free-slip boundary condition and (e) no-slip boundary condition.

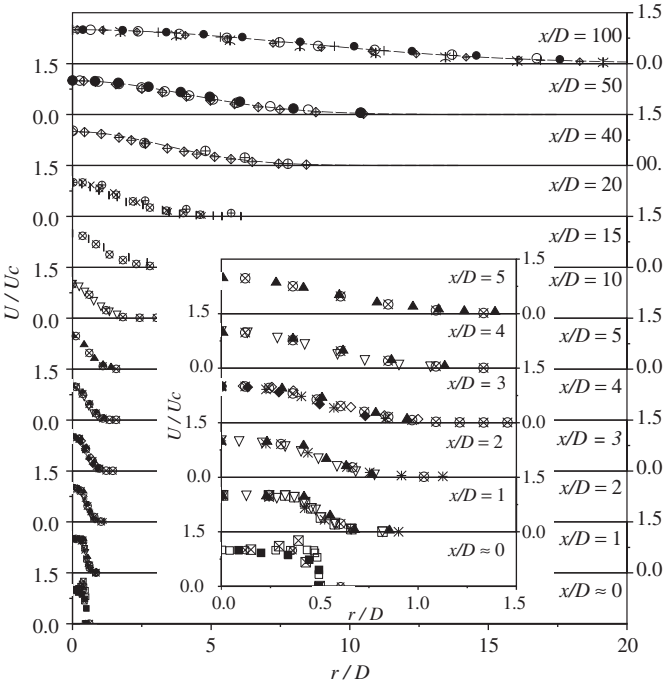

Fig. 5. Streamwise mean velocity profiles at different axial positions. Legend: discontinuous line sows a Gaussian distribution; ⟠ Wygnanski and Fiedler [17]; × Boguslawski and Popiel [146]; ▽ Quinn and Militzer [147]; + Panchapakesan and Lumley [49]; • Hussein et al., single hot-wire [51]; ○ Hussein et al., laser-Doppler anemometry [51]; | Abdel-Rahman et al. [148]; ‡ Weisgraber and Liepmann [118]; □ Mi et al., contraction nozzle [41]; ■ Mi et al., pipe nozzle [41]; ⊠ Mi et al., orifice nozzle [41]; ✳ Romano [45]; ◇ Xu and Antonia, contraction nozzle [52]; ◆ Xu and Antonia, pipe nozzle [52]; **X** Gamard et al. [133]; / Kwon and Seo [138]; ▲ Iqbal and Thomas [57]; ⊗ Fellouah and Pollard [83].

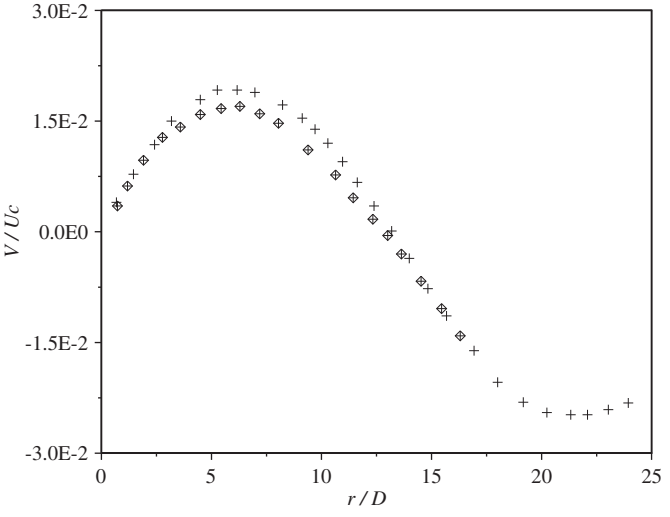

Fig. 6. Normalised radial mean velocity profiles in the far field. Legend: ⟠ Wygnanski and Fiedler [17]; + Panchapakesan and Lumley [49].

For want of investigations, the propagation of initial flow characteristics to far-field structures remains poorly understood.

Axial mean velocity profiles from the archival literature, normalised by centreline velocity and plotted against axial position, x/D, are presented in Fig. 5. The profiles are symmetric within measurement uncertainty. Hrycak et al. [48] determined experimentally and estimated analytically both the nominal and the actual length of the potential core of an axisymmetric jet. They showed that the nominal potential core length is largely independent of Reynolds number in the turbulent flow region except during transition. During laminar flow, however, it is directly proportional to Re_D.

Profiles of the mean radial velocity normalised by centreline velocity, V/U_c, from a variety of investigations are collected and presented in Fig. 6. The radial velocity results of Wygnanski and Fiedler [17] and Panchapakesan and Lumley [49] have been recalculated here from the published axial mean velocity profiles by invoking the continuity equation (with the assumption that the mean azimuthal velocity is zero). With the mean radial velocity being symmetric about the jet centreline, as shown in Fig. 6, the flow near the centreline must expand laterally outward while the surrounding fluid retracts inward; this is entrainment.

There are two theoretical models that predict the shape of the mean velocity profiles. One, based on the mixing length hypothesis, was derived by Tollmien [18]; the other, based on the assumption of a constant eddy exchange coefficient across the flow, was determined by Schlichting [50]. Such theoretical models have been used to predict basic features of the mean radial velocity. Wygnanski and Fiedler [17] showed and noted that neither of these two predicted profiles is in accord with experimental evidence over the extent of the flow; they concluded that in the outer part of the flow, Tollmien's solution agrees moderately well with experiment while in the inner part of the flow, Schlicting's solution is in good agreement. The reason these models do not work is simply that the flow physics are not captured by the supposed 'simplified' dependence on the mean velocity gradient.

The corresponding axial and radial turbulence intensity profiles at different axial positions are displayed in Fig. 7. The shapes of the profiles are nearly the same. In general, the axial turbulence intensity, u'/U_c, is greater than the transverse turbulence intensity, v'/U_c, in the streamwise direction. As will be seen later, this is because the larger structures in the flow still carry directional preference, and because the turbulence field cannot be assumed to be isotropic in this region. One of the most interesting features of the near field is the redistribution of turbulence intensity across the jet as the flow evolves downstream. Notwithstanding, the time-averaged turbulence intensities are remarkably self-similar in their shape in the far field, over $x/D \geq 60$. The intensity and shape of the transverse turbulence intensity, w'/U_c, along the streamwise direction is similar to that of v'/U_c [17,49,51]. The effects of the nozzle shape diminish drastically at approximately $x/D = 20$, as demonstrated by Xu and Antonia [52] and as shown here in Fig. 7.

The centreline axial mean velocity decays linearly with axial distance, as shown in Fig. 8. For the self-similar region, the centreline velocity variation is given by

$$\frac{U_j}{U_c} = \frac{1}{B}\left(\frac{x}{D} - \frac{x_0}{D}\right) \tag{2}$$

where x_0 is the virtual origin and B is the decay constant. Values for these quantities reported in the literature are shown in Table 1. From Fig. 8, it appears that in the intermediate field, $6 \leq x/D \leq 30$, the centreline velocity decays faster than in the self-similar region due to the flow development.

The longitudinal evolution of the turbulence intensities along the jet axis ($r/D = 0$) is provided in Fig. 9 using data from various authors (as listed in the figure caption). In the near field region, the turbulence intensities increase due to the large scale coherent motions that arise in the shear layer. As a result, their influence on the centreline intensities increase as they progress through the potential core and, eventually, coalesce. The intensities reach the nominally accepted value of about 28% for u-velocity and 20% for

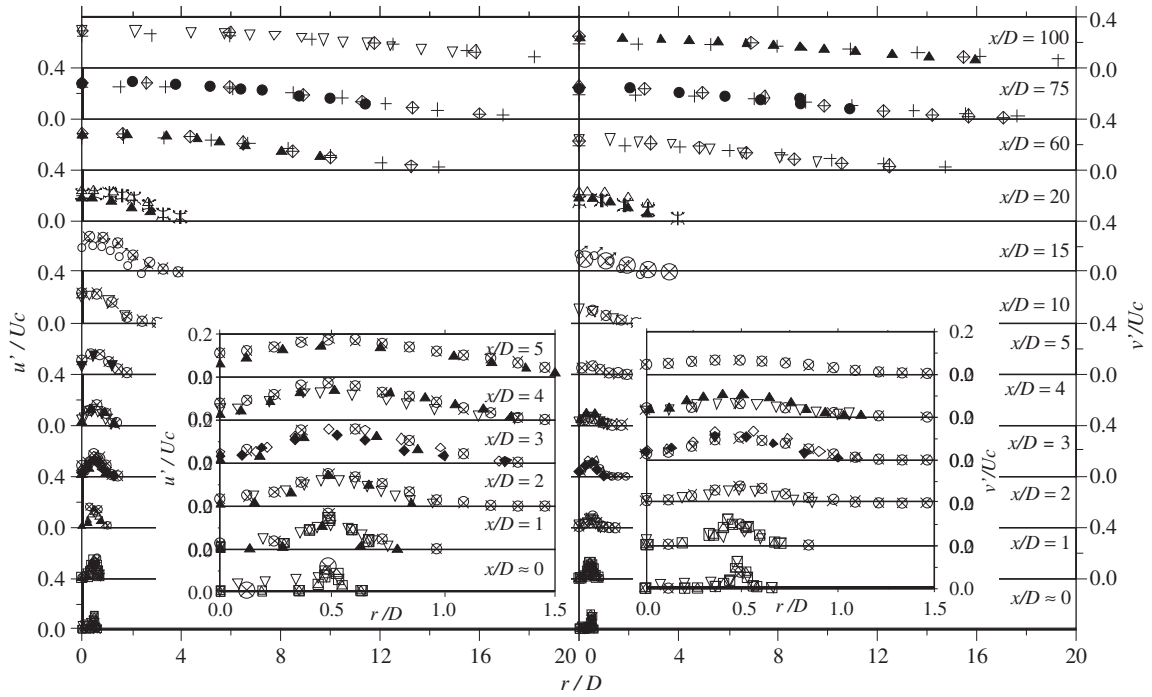

Fig. 7. Streamwise and radial turbulence intensity profiles. Legend: ⊕ Wygnanski and Fiedler [17]; ⊠ Chevray and Tutu [149]; × Boguslawski and Popiel [146]; ▽ Quinn and Militzer, contraction nozzle [147]; △ Quinn and Militzer, sharp nozzle [147]; + Panchapakesan and Lumley [49]; • Hussein et al., single hot-wire [51]; ‡ Weisgraber and Liepmann [118]; ◇ Xu and Antonia, contraction nozzle [52]; ♦ Xu and Antonia, pipe nozzle [52]; ▲ Iqbal and Thomas [57]; ⊗ Fellouah and Pollard [83].

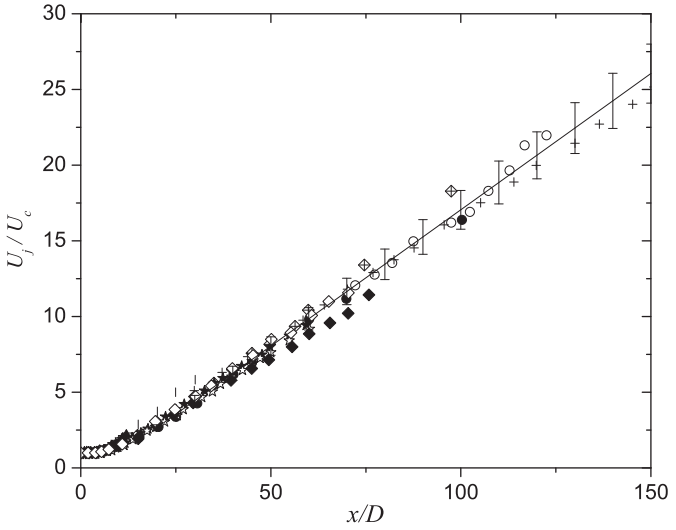

Fig. 8. Axial decay of centreline mean velocity (error bar: ±8%). Legend: ⊕ Wygnanski and Fiedler [17]; × Boguslawski and Popiel [146]; + Panchapakesan and Lumley [49]; • Hussein et al., single hot-wire [51]; ○ Hussein et al., laser-Doppler anemometry [51]; | Abdel-Rahman et al. [148]; ◇ Xu and Antonia, contraction nozzle [52]; ◆ Xu and Antonia, pipe nozzle [52]; ⋆ Quinn, sharp nozzle [42]; ☆ Quinn, contoured nozzle [42]; ▲ Iqbal and Thomas [57].

v-velocity at $x/D \approx 30$ [17]. From this figure, it is observed that during jet development the magnitude of v' is always less than that of u'. In the far field, the turbulence intensity remains constant. Quinn [42] showed that the turbulence intensities in the sharp-edged orifice jet reach a maximum before the turbulence intensities in the contoured nozzle jet (which are generally lower in magnitude); this is a reflection of the increased mixing in the case of the sharp-edged orifice jet. The plateau, where the turbulence intensity is constant, is attained faster in a contraction nozzle than for a pipe jet. This trend, in conjunction with the decay of centreline velocity, suggests that the sharp-edged orifice jet becomes self-similar more rapidly than the jet that issues from a pipe. In each of these flows, the radial turbulence intensity, v'/U_c, becomes steady farther downstream than the axial turbulence intensity, u'/U_c. The data suggest that the effect of the initial condition seems not to affect the development of turbulence intensity.

Reynolds shear stresses, normalised by the square of centreline velocity U_c^2, are presented in Fig. 10. The greatest exchange of momentum – a process which involves large scale vortices – occurs in the jet shear layer. The maximum Reynolds stress is shifted away from the centreline with downstream distance in accord with the diffusion of the maximum gradient in mean axial velocity (and in accord with the thin shear layer approximation). Citriniti and George [53] used 138 synchronised hot-wire

Table 1
Centreline mean velocity parameters (see Eq. (2)).

Authors	Nozzle	x/D	x_0/D	B
Wygnanski and Fiedler [17]	Contraction	<50	3	5.7
		>50	7	5.0
Panchapakesan and Lumley [49]	Contraction	30–160	0	6.06
Hussein et al. [51]	Contraction	30–120	2.7	5.9
Weisgraber and Liepmann [118]	Contraction	17–27	0	6.7
Ferdman et al. [70]	Pipe	≥ 15	2.5	6.7
Mi et al. [41]	Contraction	0–64	3.5	4.48
Xu and Antonia [52]	Contraction	20–75	3.7	5.6
Quinn [42]	Sharp-edged orifice	18–55	2.15	5.99
	Contraction	18–55	3.65	6.1
Fellouah et al. [84]	Contraction	15–29	2.5	5.59

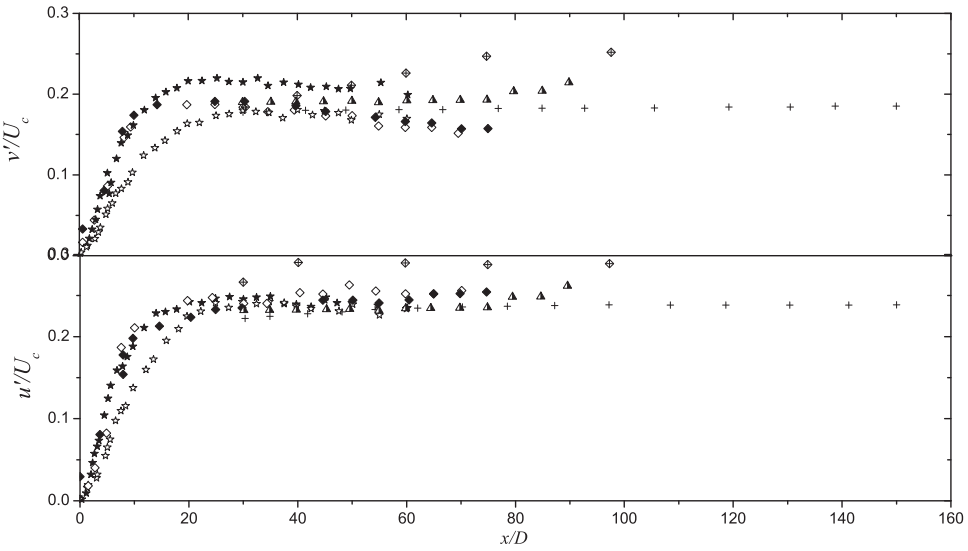

Fig. 9. Evolution of centreline turbulence intensities. Legend: ⊕ Wygnanski and Fiedler [17]; + Panchapakesan and Lumley [49]; ◇ Xu and Antonia, contraction nozzle [52]; ◆ Xu and Antonia, pipe nozzle [52]; ⋆ Quinn, sharp nozzle [42]; ☆ Quinn, contoured nozzle [42]; ▲ Burattini et al. [75].

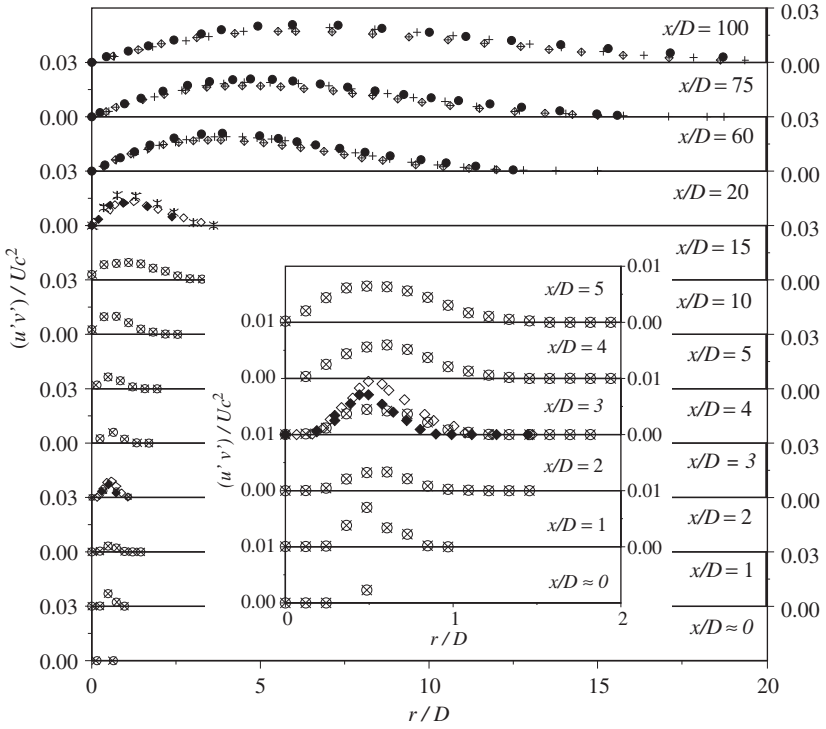

Fig. 10. Reynolds shear stress at different positions (normalised by U_c^2). Legend: ⟡ Wygnanski and Fiedler [17]; + Panchapakesan and Lumley [49]; • Hussein et al., single hot-wire [51]; ‡ Weisgraber and Liepmann [118]; ◇ Xu and Antonia, contraction nozzle [52]; ◆ Xu and Antonia, pipe nozzle [52]; ⊗ Fellouah and Pollard [83].

measurement channels, for a jet with $Re_D = 80,000$ and at $x/D = 3$, and applied the proper orthogonal decomposition to reconstruct the global velocity field. From their data, it was found that longitudinal counter-rotating vortices create alternating positive and negative radial fluid advection patterns. It was furthermore concluded that the life-cycle of the large scale structures includes intra-vortex ring braids which appear as counter-rotating pairs, that the intra-vortex region is a high-strain field, and that the braids are integral to the entrainment process. This was confirmed in an LES study of round jets with and without swirl by McIlwain and Pollard [54]. These findings on fluid structures are described thoroughly in Section 4.6.

The statistics revealed a close coupling between the mean velocity distribution and both the turbulence intensity and Reynolds shear stress. The location of the peaks in the turbulence intensity profile corresponds to the local maximum of the mean velocity gradient. The mean velocity seems to evolve to the self-similar state more quickly than do the turbulence intensities. In Wygnanski and Fiedler [17] the self-similarity is described as a state in which the components of flow turbulence are all in equilibrium. Since energy is transported from the mean motion to fluctuating velocities, similarity must be reached through a series of steps. First, the mean velocity becomes self-similar, then do the second order statistics and the third order, and so on [4].

Efforts to characterise, to generalise the nature of the flow from a round jet have progressed to, first, explorations of similarity, and further to discovery of more complex flow features (as will be seen in here, in ensuing sections). The accumulation of results presented in the preceding figures confirms that, when suitably normalised, data obtained from this variety of investigations are repeatable. While the basic features of the flow may be revealed using measurement and characterisation techniques, higher-level questions are raised. An appropriate exploratory enquiry might be: What specific characteristics of the jet enable it to behave as it does? With the arrival of more sophisticated experimental and computational techniques, answers to this question are more readily forthcoming. Early advancement in exploration was stymied somewhat with the understanding that flow from the jet is not limited to the regions of the centreline, the shear layer, and the outer layer. The surrounding space and the ambient fluid, as first uncovered by Seif [36] and later by [55] and George et al. [56], are vitally important in jet flow development; and so, entrainment in jet flows must also be understood.

4.2. Entrainment

In this section we focus on entrainment—the engulfment of surrounding (ambient) fluid that maintains the momentum flow rate but causes the mass flow rate of the jet to increase with distance from the jet origin.

Measurements of growth of the jet half-radius, $r_{1/2}$ with downstream distance are plotted in Fig. 11. The mean spread rate of $r_{1/2}$ that increases linearly beyond the potential core ($x/D \approx 15$) is fitted to the equation

$$\frac{r_{1/2}}{D} = A\frac{x}{D} - B \tag{3}$$

Some investigators' constants (A and B) are shown in Table 2. It is noted that the results of Iqbal and Thomas [57] differ significantly in the spread rate; it is not clear to the current authors why these differences exist.

In both Capp [55] and George et al. [56] it was hypothesised that the momentum lost to recirculation in the late intermediate and far-field regions of the jet was caused by an insufficiently large jet facility. This claim was later verified in both Capp et al. [58] and Hussein et al. [51]; in both papers, a similar nozzle and a much larger room than that of Wygnanski and Fiedler [17] were used to create, as close as possible, the condition of a jet in an infinite environment. A criterion to relate jet mass flux and room size to the expected momentum loss was derived in George et al. [56].

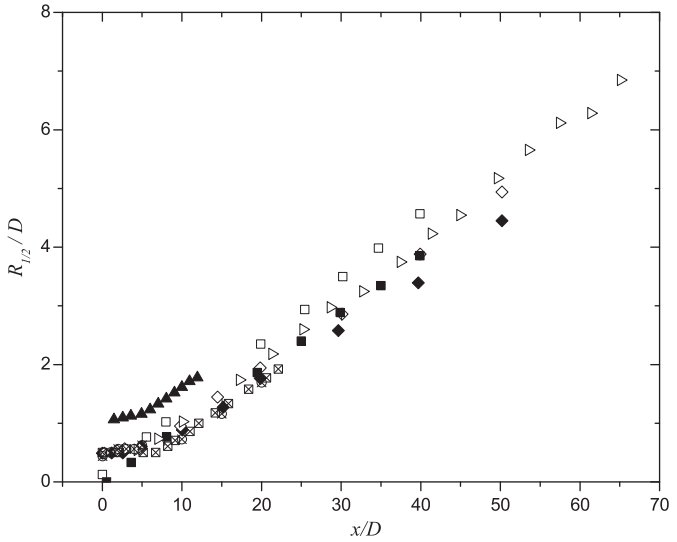

Fig. 11. Axial evolution of the jet width. Legend: ⊠ Quinn and Militzer [147]; | Abdel-Rahman et al. [148]; □ Mi et al., contraction nozzle [41]; ■ Mi et al., pipe nozzle [41]; ▷ Mi et al., orifice nozzle [41]; ◇ Xu and Antonia, contraction nozzle [52]; ◆ Xu and Antonia, pipe nozzle [52]; ▲ Iqbal and Thomas [57]; ⊠ Shineeb et al. [140]; ⊗ Fellouah and Pollard [83].

Table 2
Linear fit constants (see Eq. (3)).

Authors	Nozzle	*A*	*B*
Panchapakesan and Lumley [49]	Contraction	0.096	
	Contraction	0.095	
Xu and Antonia [52]	Pipe jet	0.086	
Fellouah and Pollard [83]	Contraction	0.097	0.259

To measure the entrainment of a round jet, Ricou and Spalding [19] devised and constructed an ingenious apparatus composed of a jet enshrouded by porous cylinders through which pressurised air was supplied to match the volumetric flow rate of air that would have been entrained in the absence of the cylinders. It was possible to match the entrainment flow rate by recognising that, without the cylinders, the large reservoir of ambient fluid would be at uniform pressure (except in the vicinity of the jet axis). The presence of the porous cylinders (without any air supply) would have impeded the radial inflow of ambient air; as a result, the fluid within the enclosure but outside of the cone of the jet would have been forced to flow axially. The corresponding axial pressure gradients would not have been zero, and could be measured. In the apparatus of Ricou and Spalding [19], the flow rate through the porous enclosure was set so that there would be no axial pressure gradient. This flow rate was measured, and presumed to be equal to the entrainment flow rate of an enclosure-free (normal) jet.

In the experiment by Ricou and Spalding [19], various effects were measured over the Reynolds number range $500 \le Re_D \le 80,000$ and over the axial range $2.4 \le x/D \le 418$. As a result of this work, an entrainment law that relates mass flow rate, jet momentum, axial distance, and air density was deduced; these effects are related by the expression

$$\frac{m}{x(M\rho_1)^{1/2}} = K_1 \tag{4}$$

where m is the streamwise mass flow rate of the jet, x is the axial position, M is the excess momentum flux of the jet, ρ_1 is the density of the surrounding fluid, and K_1 is the entrainment constant. In a preliminary investigation, the effect of Reynolds number on the entrainment ratio (the ratio of the jet orifice mass flow rate to the entrainment mass flow rate, m_1/m_0) was examined over the entire Reynolds number range of the experiments. It was found that the ratio m_1/m_0 was approximately constant for Reynolds numbers greater than 25,000. As a result of this finding, Ricou and Spalding [19] elected to conduct the remainder of their experiments over $Re_D \ge 25,000$, which is beyond the mixing transition Reynolds number of approximately 20,000 proposed by Dimotakis [59] (a theory that had not yet been proposed). Even before these efforts, Donald and Singer [60] reported that entrainment in the region $x/D < 14$ was not significantly different from that in the region of fully developed flow; this finding, however, is not in accord with those data of Ricou and Spalding [19].

Hill [61] measured the local entrainment rate in the initial region of axisymmetric air jets by an adaptation of the porous wall technique used by Ricou and Spalding [19] in which the jet was directed through an open-ended short chamber that was open to the atmosphere. Results showed that the

> local entrainment rate, which is independent of the nozzle Reynolds number for values of $Re_D > 60,000$, is strongly dependent upon the axial distance. At an axial distance of one nozzle diameter the local entrainment rate is only about one-third of that in the fully developed jet; the entrainment rate increases with increasing axial distance to reach the fully developed value at an axial distance of about thirteen nozzle diameters [61].

Broad appreciation for the jet's interaction with its environment is derived from an understanding of entrainment. It is a first order effect for free shear flows and yet a main parameter that is critically important in many applications—for example, mixing and diffusion of species that may be either benign or not, to enhance combustion, and so on. Mixing in the context considered here is between the jet source material and the material entrained from the reservoir into which the jet is injected. As will be noted below, vorticity distribution in the jet is a key ingredient to entrainment—both are related to the distribution of length scales in the flow. However, before attending to length scales, attention is turned to the effects of initial conditions.

4.3. Initial conditions and similarity

The effects of initial conditions and the supposed universal character of self-similarity have been the subject of considerable research over the years. Bradshaw [62] considered the effects of initial conditions on some characteristics of the jet and its shear layer. Specifically, the nozzle boundary layer thickness was varied by fastening parallel sections of various pipe lengths to the end of the nozzle. For the circular jet, this would result in alteration of the vortex rings emanating from the nozzle. Mach number, Reynolds number, and nozzle boundary layer effects on noise from the jet were also examined; Bradshaw concluded that a significant rise in the noise-emission coefficient below $Ma \approx 0.5$ was most likely a Reynolds number effect [62]. However, Reynolds number dependence of other statistics was not reported.

Lai [63] deduced the 'preferred mode' of a jet (a frequency at which an axisymmetric disturbance is amplified and maximised in the jet, see [64], that is characterised by the Strouhal number) from measurements of the frequency spectra of the streamwise turbulent velocity. The results show that the preferred Strouhal number increases with the Reynolds number for the fully developed laminar exit condition while it is independent of Reynolds number for a fully developed turbulent exit condition. The concept of 'modes' introduced here is in the context that a flow

is excited at its origin. As will be introduced later, modes may be also used to reconstruct a turbulence signal.

Turbulence and pressure measurements were taken in the initial regions of round single jets in Ko and Davies [65] and in round co-axial jets in Ko and Kwan [66]. In Ko and Davies [65], results (which were primarily confined to the potential core) showed significant dependence of pressure fluctuations (and vortices) and turbulence fluctuations on jet velocity; measurements were taken for $Ma < 0.45$ (which corresponds to $Re_D < 190,000$). In Ko and Kwan [66], turbulence and pressure measurements were taken from co-axial jets of three different mean velocity ratios. Investigators were interested in flow evolution in the initial field of the co-axial jets; however, because of similarity with single jets, they found that the complicated flow structure of the co-axial jets could be related to and described by the structure of single jets. Again, keep in mind that these studies were conducted for fairly high Reynolds numbers.

Capp et al. [58] and Hussein et al. [51] observed significant differences between laser-Doppler anemometry (LDA) and stationary hot-wire (SHW) measurements, especially in the higher-order moments [58]. Meanwhile, the flying hot-wire (FHW) measurements of triple moments taken in the experimental facility of Hussein et al. [51] matched closely with LDA measurements. In regions of elevated turbulence intensity, SHW measurements suffered due to cross-flow, rectification, and data drop-out errors. The LDA and FHW results, on the other hand, were confirmed to be consistent with the equations of motion. Similar conclusions were drawn in a parallel study by Panchapakesan and Lumley [49]; some discrepancies in the results, however, were attributed to differences in Reynolds numbers and initial conditions of the flows. In the experiments of Capp et al. [58] and Hussein et al. [51], the nozzle outlet had a top-hat velocity profile with turbulence intensity of 0.58% and $Re_D = 95,500$; whereas in Panchapakesan and Lumley [49], the top-hat velocity profile had a turbulence intensity of $O(0.01)\%$ and $Re_D = 11,000$.

In contrast to the classical treatment of Hinze [38], a theoretical analysis was suggested by George [4] that turbulent flows can become asymptotic to a variety of self-similar states that are determined by initial conditions. Regarding both passive scalar and vector quantities, there have been extensive efforts to clarify the classical hypothesis of universal similarity and to reconcile it with the analytical result of George [4]. Review articles on self-similarity of the scalar field provide inconsistent results. For example, the conclusions of Richards and Pitts [40] support the hypothesis of universal self-similarity of a jet flow; the asymptotic state of the scalar field (as characterised by mean spreading rate, centreline mean decay rate, and locally normalised root-mean-square fluctuations) has minimal dependence on initial conditions. Meanwhile, Dowling and Dimotakis [15] found a Reynolds number dependence of the far-field decay rate of the mean concentration field and the radial distribution of the root-mean-square concentration fluctuations. In a comparison of flow from an axisymmertric jet ($Re_D = 16,000$) with two different initial conditions, Mi et al. [41] examined the flow field over $0 \le x/D \le 70$ to verify the analytical result of George [4]. By comparing two jet flows (one with a top-hat, the other with fully-developed pipe flow initial conditions), it was confirmed that turbulent scalar properties throughout the jet flow are dependent on initial conditions. Furthermore, it was re-affirmed that a universal asymptotic state of turbulence that is independent of initial conditions is unlikely to exist [41].

The classical hypothesis of universal self-similarity has also been questioned regarding velocity statistics. Efforts to understand the effects of initial conditions on flow development in a jet are not new; Bradshaw [62] used a round jet and made measurements in the quasi-plane region of the mixing layer (within the first few diameters downstream of the nozzle) to summarise the effect of initial conditions on the development of a free shear layer. In many other investigations, the focus was on development of the jet as a whole. More recently, in a direct numerical simulation (DNS) of a round jet with $Re_D = 2400$, Boersma et al. [67] found that different nozzle outlet conditions would affect the mean and fluctuating velocities. Although the measurement range of this study ($x/D \le 42$, due to computational limitations) did not extend into the truly self-similar region, these results support the hypothesis of George [4] that the asymptotic state of the flow will vary with initial conditions. It is critically important to note, however, that Re_D used by Boersma et al. [67] was well below the mixing transition and the near field flow is laminar-like.

In the near field, Martin et al. [68] studied the effects of perturbations on the evolution of three-dimensional structures in axisymmetric co-flowing jets at $Re = 1000$. They also considered an inviscid computation based upon the Biot–Savart rule. They considered mild acoustic sinusoidal forcing of the flow that issued from a slightly corrugated nozzle and found the Kelvin–Helmholtz-like instabilities to be interconnected by streamwise braids. In discussions on the mechanisms for re-organisation of jet vorticity, it was noted that at low to moderate Reynolds numbers, inviscid mechanisms dominate the flow. For the mixing transition Reynolds number range of $O(20,000)$, Olsson and Fuchs [69] conducted an LES of the near field region ($3 \le x/D \le 9$) of a round jet. In this work, mean velocities, turbulence intensities, Reynolds shear stresses, energy spectra, and Taylor microscales were monitored for six different flow cases to study the effects of Reynolds number (and computational parameters). Reynolds number dependence in the simulation range, $10,000 \le Re_D \le 50,000$, was demonstrated but not clearly explained. More recent experimental and computational works have extended the axial range for investigations into the effects of initial conditions. Ferdman et al. [70] used a cross-wire to investigate the effect of initial mean velocity profiles on downstream mean and turbulence statistics. Comparing their own results for turbulence quantities from two different pipe-jets with $Re_D = 2400$ over $0 \le x/D \le 80$ with results obtained by other researchers, Ferdman et al. [70] found that far-field decay rates of pipe-jets are less than those with initial top-hat velocity profiles.

Over a 7-year time span from the year 2000, Antonia's research group at the University of Newcastle conducted several studies on the effects of initial conditions on circular jets. Romano and Antonia [71] observed different values of v'/u' and non-negligible differences in small scale characteristics in the far fields of circular air and water jets with slightly different initial conditions. Antonia and Zhao [72] compared energy spectra and velocity fluctuations over the range $0 \le x/D \le 50$ for two jets, one with a fully developed pipe-flow outlet and the other with a laminar top-hat profile, both at $Re_D = 37,000$. It was found that the two jets behaved differently in the near and intermediate fields, but reached the same state of self-preservation at approximately the same x/D; spectra of axial and radial velocity fluctuations were found to collapse over the range of scales from the Kolmogorov length scale to their chosen integral scale. However, Xu and Antonia [52] report that, for the same two jet outlet conditions of Antonia and Zhao [72] but for a larger Reynolds number, $Re_D = 86,000$, the mean velocity and Reynolds stresses that result from the use of the contraction nozzle develop and approach self-similarity faster than for the pipe-flow jet. This was attributed to differences in turbulent structures in both the near and far fields of both flows, as implied from spectra, length scales, development of turbulence intensities, and profiles of the Reynolds stresses. Instead of varying the Reynolds number, Burattini et al. [73,74] placed grids at the nozzle outlet to alter the jet initial conditions, causing an injection of small scales into the flow. As a result,

it was possible to investigate the manner in which initial development and large-scale instabilities of a round jet are affected by small-scale injection of turbulence energy [73]. Three jet flows were studied over $x/D \leq 30$ at $Re_D = 49,000$: one without a grid, two others each with a different grid. It was found that, as a consequence of weaker coherent structures, the perturbed jets showed decreased growth rates and extended regions of streamwise decay. It was furthermore demonstrated that for this large Reynolds number, the velocity field in the near to intermediate field (NIF) is directly affected by inlet conditions (unperturbed top-hat versus grid-perturbed top-hat profiles). It is uncertain whether these phenomena are universally true. In light of the assertion that a mixing transition to a fully-developed turbulent flow requires a minimum outer-scale Reynolds number of $O(10^4)$ [59], dependence of the NIF development on initial conditions is not fully understood. It would be appropriate to investigate the effect of inlet conditions, by varying Re_D and inlet velocity profiles, on the development in the near to intermediate field of a round free jet.

Burattini et al. [75] examined the similarity in the far field of a turbulent jet by using hot-wire anemometry techniques. They focussed on the similarity of the structure function equation along the jet axis and found that the Taylor microscale is the relevant characteristic length scale. They noted that energy structure functions along the jet axis supported this finding—that is, when normalised by the Taylor microscale, λ, and the mean turbulent energy, $\langle q^2 \rangle$, the energy structure functions collapse upon each other over a wide range of scales. It was also found that the best collapse occurs over the dissipative range when Kolmogorov variables are used [75]. Moreover, the best collapse at large separations was produced using mean turbulence energy and integral length scales. To understand the control of turbulence, Rajagopalan and Antonia [76] used hot-wire anemometry and discovered that in order to achieve passive enhancement of turbulence, the potential core must be perturbed. A hybrid technique that combines the features of active and passive techniques has been shown to be useful in suppressing large structures [76].

In a comparative review of several different studies on turbulent jets and plumes, Carazzo et al. [77] proposed that, in an appropriate parameter space for entrainment, global evolution toward self-similarity follows a universal route. This distinction from the hypothesis of local self-similarity postulated by George [4] requires qualification. That is, over a sufficiently large range of x/D, knowledge is needed of the evolution of dynamical variables and entrainment as functions of x/D. Evolution with downstream distance was proposed to be the major effect on the route to global self-similarity; however, clear understanding of the effects of other experimental parameters on evolution will be required.

In Uddin and Pollard [43], the existence of self-similarity, the virtual origin, and a physically relevant length scale were investigated. The effect of initial conditions on a spatially developing co-flowing jet was studied using LES. The flow configuration, with a nominal Reynolds number of $Re_D = 7300$ and a co-flow inner-to-outer velocity ratio of 11, was a very close approximation to that of Nickels and Perry [78]; the interrogation region was $0 \leq x/D \leq 90$. Four different inlet conditions were used in which both the mean and fluctuating velocity profiles, obtained from different assumptions, were considered; as a result, it was possible to associate causal relationships between types of initial conditions and downstream effects. It was found that mean centreline velocity decay and radial mean velocity profiles were insensitive to initial conditions, while turbulence statistics were strongly affected by initial conditions. The Reynolds stresses were found to be extremely sensitive to turbulence intensity of the inlet conditions; the Reynolds numbers of the flow considered were less than required for the mixing transition [59].

Uddin and Pollard [43] argue that while self-preservation of the mean velocity profiles should be demonstrable with prudent choices of length and velocity scales, there is no definitive evidence that a similar conclusion can be drawn with regard to the higher moments. Although the choice of length and velocity scales appears to be important [5,79], the commonly used length scale appears to be merely arbitrarily convenient rather than physically relevant. With their simulation results, Uddin and Pollard [43] proposed that the variance of the local velocity distribution, the effective jet width Δ, is a better choice of length scale; this kinematic length scale reflects the effect of the formation of the viscous layer at the nozzle exit. It is given by

$$\Delta^2 = \frac{\int (U-U_1) r^2 \, dr}{\int (U-U_1) \, dr} \tag{5}$$

where U_1 is the external or co-flow velocity (of course, for a free jet $U_1 = 0$). This kinematic length scale reflects the effect of the formation of the viscous layer at the nozzle exit.

This work is considered to be a step beyond that of Boersma et al. [67]. The findings of Uddin and Pollard [43] are summarised here:

- Mean statistics appear to be insensitive to initial conditions.
- Turbulence statistics are significantly affected by the initial conditions.
- Reynolds shear stress has weakest dependence on inlet conditions, streamwise normal stress has the strongest.
- As the flow evolves downstream, the effect due to variation of initial conditions appear to be amplified.

The utility of the new scaling factor was only tested against jet flows with different inlet conditions. Reynolds number effects are unknown. With regards to arguments about the role of the virtual origin, one must recall the argument of George [4] that the self-preserving state depends on initial conditions, and cannot be assumed, as it had been previously, to grow from a point source of momentum [79].

In light of the question regarding the existence of a universal self-similarity in the far field, investigations into the far-field effects of initial conditions were well warranted. Experiments of Dimotakis et al. [80] using laser-induced fluorescence (LIF) reveal qualitative differences in the scalar field for jet flows below and above the transitional $Re_D \approx 10^4$, as put forth in Dimotakis [59].

This mixing transition can be seen in Fig. 12; unmixed reservoir fluid is seen throughout the turbulent region (to the jet axis) in the lower Reynolds number flow (Fig. 12a), while a smooth variation of jet-fluid concentrations is seen in the higher Reynolds number flow (Fig. 12b). A number of investigations into the Reynolds number effects on the scalar field include those of Dowling and Dimotakis [15], Miller and Dimotakis [81], and Liepmann and Gharib [82]. A brief review of near and intermediate field studies of flow development is presented next.

The NIF was measured experimentally and reported in Fellouah and Pollard [83] and Fellouah et al. [84] to investigate Reynolds number effects over the range spanning the mixing transition. From the velocity spectra, it was found that the inertial subrange emerged at Reynolds numbers above $Re_D \approx 20,000$, where the energy of the large scale turbulence (with low wave numbers or frequencies) is carried directly to the dissipative range of scales. It was deduced that the mixing transition occurred at the emergence of the inertial subrange rather than at the transition from the inertial to the dissipation range. Spectra from these studies revealed that accelerated development of the jet flow, either axially or radially, favours the emergence of the inertial subrange. In this work, the relationships between the various length scales in the near field were illustrated.

Furthermore, two features were demonstrated: firstly, that the ratio of the laminar to the viscous length scales exceeds unity in the region beyond the potential core; and, secondly, that the Kolmogorov, Taylor, and viscous length scales all decrease in magnitude with increasing Reynolds number. These confirm the arguments of Dimotakis [59] as they are applied to the far field of a jet. These scales appear to be only weakly dependent on radial position; the ratio $Re_T/Re_\delta^{1/2}$ varies non-linearly across the jet radius [84,83].

In this section, it is clear that initial and boundary conditions play a significant role in jet development and that routes to similarity, at least with respect to mean and second order moments should be appropriately scaled.

4.4. Length scales

The impact of initial conditions on the downstream development of a flow is significant even in the far field [4]. This was confirmed by Mi et al. [41] who considered two jets that originated from a smooth contraction and a long pipe, and found that the scalar field differences in statistics may be related to the differences in the underlying structure in the near field of the jet. Clearly, an orifice plate will generate a circular jet with an initial flow condition that is vastly different from that generated by other types of nozzle.

The current view of turbulence is that it is a multi-scale phenomenon in both length and time; however, identification of appropriate (or definitive) length scales is unclear. By including information about the way in which energy is contained within and transferred among the different scales of motion, Ewing et al. [85] claimed that equilibrium similarity solutions for a finite Reynolds number jet are allowed by the governing equations for the two-point velocity correlations in the far field of the axisymmetric jet. Moreover, they note:

> The two-point velocity correlation can be written as the product of a scale that depends on the downstream position of the two points and a function that only depends on the similarity variables. Physically, this result implies that the turbulent processes producing and dissipating energy at the different scales of motion, as well as transferring energy between the different scales of motion, are in equilibrium as the flow evolves downstream [85].

A proposal based on the relative magnitude of dimensional spatial scales for the relative sizes of various length scales was offered by Dimotakis [59]. He began with the theory presented by Kolmogorov [3,86], and focussed on different regions within the spectra of longitudinal velocity. That is, at low wave number the length scale is the local time-averaged diameter, δ, while at the highest wave number the Kolmogorov length scale, λ_K, is appropriate. Between these two limiting cases, he introduced the viscous length scale, $\lambda_v = 2\pi/\kappa_1$, which is the lower boundary of the inertial sub-range. It is estimated using the wave number, κ_1, where the energy spectrum deviates from the $-5/3$ slope which, from the spectral measurements, happens for $\kappa_1\lambda_K = 1/8$. Other length scales used in the literature are the Taylor microscale, λ_T, and the laminar length scale, λ_L (see Saddoughi and Veeravalli [87] and Dimotakis [59]). The laminar length scale is the region where the inertial range begins; it separates the energy containing ranges from the inertial ranges. Zhou [88] noted that the Liepmann–Taylor microscale essentially describes the internal laminar vorticity growth layer generated by viscous shear along the boundaries of a large scale feature of size δ. Dimotakis claimed, in a private communication with Liepmann, that the Liepmann–Taylor microscale can also be understood as the internal viscous shear-layer thickness associated with a large scale motion, spanning the full transverse extent, δ, of the flow. As such, it is the smallest scale generated by a δ-size eddy

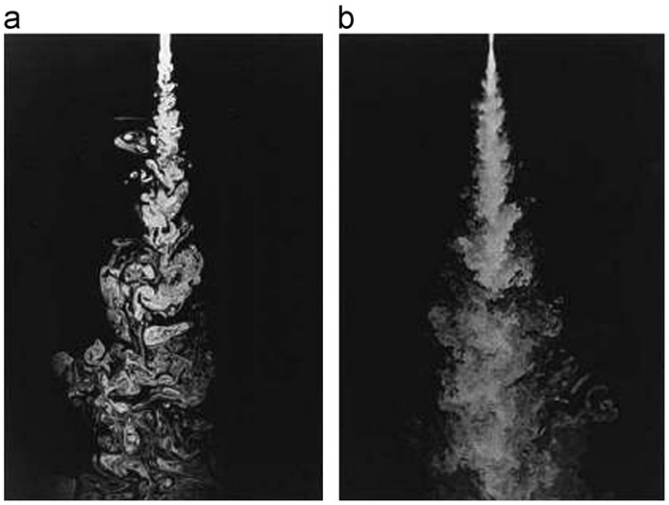

Fig. 12. Jet-fluid concentration in the plane of symmetry of a round jet. (a) $Re_D \approx 2500$; $(0 \le x/D \le 35)$. (b) $Re_D \approx 10,000$; $(0 \le x/D \le 200)$. Reprinted with permission, from [80]; copyright © 1983, American Institute of Physics.

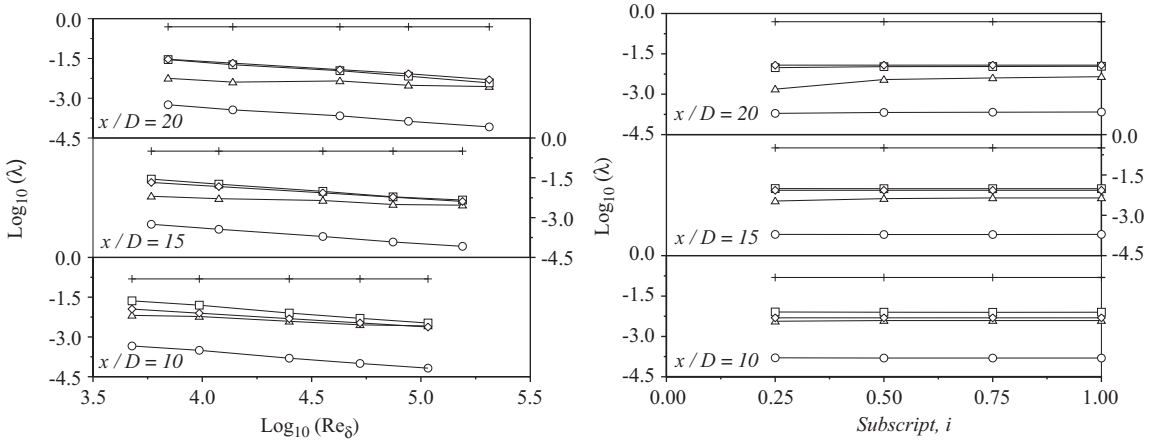

Fig. 13. Length scales as a function of Reynolds number at the jet axis. Legend: ○ : λ_K, △ : λ_T, ◇ : λ_L, □ : λ_μ. Reprinted with permission, from [83]; copyright © 2009, American Institute of Physics.

(or sweep) and defines the range of scales directly connected to outer-scale dynamics by viscous action. Dimotakis concluded that the manifestation of this transition may depend on the particular flow geometry and is a universal property of turbulence; he furthermore argued that a necessary condition for both fully developed turbulence and the Kolmogorov inertial-range similarity ideas to begin to apply is the existence of a range of scales that are uncoupled from the large scales, on the one hand, and free from the effects of viscosity, on the other [59]. The relation $\lambda_L/\lambda_\nu > 1$ should hold; this requires a minimum Reynolds number of $O(10^4)$ or a Taylor Reynolds number of $O(10^2)$. Antonia et al. [89] suggested that although self-preservation is reached on the basis of mean velocity, turbulence intensities, and higher order turbulence moments, this may not be the case for the dimensional spatial scales.

The development of the five length scales versus $\log_{10}(Re_\delta)$ at different axial and radial locations was investigated experimentally by Fellouah and Pollard [83]; results are shown in Fig. 13. Their results confirm the relation given by Dimotakis [59] that $\lambda_K < \lambda_T < \lambda_\mu$ and $\lambda_L < \delta$. It is apparent that all scales below δ decrease with increasing Re_δ, irrespective of axial location. At locations across the jet radius, again irrespective of axial location, these length scales vary only slightly, if at all. Additionally, the relation between λ_L and λ_μ is affected by the variation in axial positions (as shown in Fig. 13). When the Reynolds number or the axial distance is increased, the relation between λ_L and λ_μ changes; for small Reynolds numbers or for axial positions close to the nozzle exit, the viscous length scale approaches the laminar length scale, $\lambda_\mu \approx \lambda_L$. As Re_δ exceeds $\sim 10^4$, the λ_L and λ_μ scales should diverge, according to Dimotakis [59]. The results of Fellouah and Pollard [83] do not support this conclusion, at least over the Re_δ range and axial extent of measurements considered. However, their data reinforce the spatial variability of the length scales along the jet centreline, thus, the local nature of the mixing transition. Using additional scaling arguments, Dimotakis [59] concluded that a necessary condition for fully-developed turbulence and the Kolmogorov inertial range similarity to apply is the existence of a range of scales that are uncoupled from the large scales and are free from the effects of viscosity. Therefore, the relation $\lambda_L/\lambda_\mu > 1$ should hold.

The growth of the Taylor and Kolmogorov microscales as a function of axial distance from the jet, as shown in Fig. 14, is linear for $x/D \geq 15$ as given by

$$\frac{\lambda_T}{D} = A\, Re_\delta^{-1/2} \frac{x}{D} \tag{6}$$

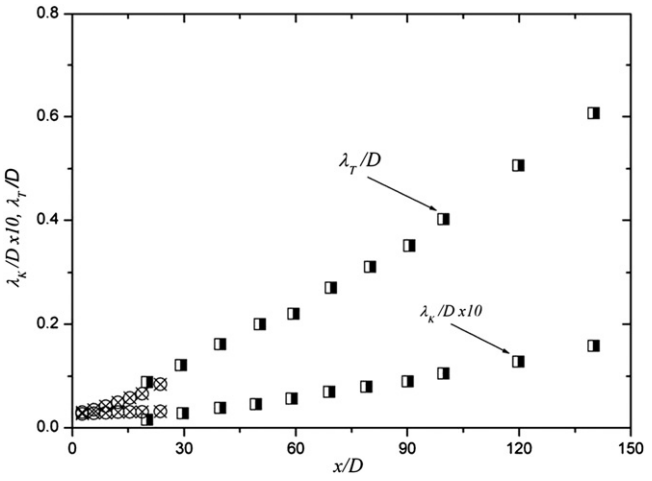

Fig. 14. Growth of the Taylor and Kolmogorov microscales with axial distance. Legend: ◨ Antonia et al. [89]; ⊗ Fellouah and Pollard [83].

and

$$\frac{\lambda_K}{D} = (B\, Re_\delta^3)^{-1/4} \frac{x}{D} \tag{7}$$

The constants of these equations were found to be $A=0.88$ and $B=48$ by Antonia et al. [89], and $A=0.79$ and $B=160$ by Fellouah and Pollard [83].

The distribution of length scales in a jet, while informative, continues to hide the physical characteristics of the fluid elements that create them. It has been noted above that the mixing transition is local and that the Kolmogorov, Taylor, and viscous length scales all decrease in magnitude with the local Reynolds number and appear to be only weakly dependent on radial position. It is no simple task to identify and nominate appropriate length scales—scaling depends on viewpoint, purpose, and the scale being considered. It thus appears to be an accepted circular analysis that the choice of length scale depends, in part, on the observed scale. Regardless, it is clear that the only tenable length scales have a physical basis.

4.5. Spectral analysis

A turbulent velocity signal is rich in frequencies. By this we mean that the signal is a measure of the contributions made by fluid parcels or eddies of different sizes, each of which provides its own contribution to the final time series. Signal analysis may entail performing spatial and auto correlations or examination of skewness or flatness of the signal; of equal utility is the energy spectrum, which identifies contributions to the signal from various length scales. A normalised (by Kolmogorov scales) power spectrum $E_{11}k_1(\epsilon\nu^5)^{-1/4}$ versus $k_1\eta$ provides information on what length scales contribute what energy. However, there is a large body of evidence to suggest that one-dimensional spectra are somewhat universal once the effects of the largest scales are ignored, see Saddoughi and Veeravalli [87].

The Reynolds number seems to affect the u-velocity spectra, as demonstrated in Fellouah and Pollard [83] and shown here in Fig. 15. In the initial sub-range of the spectrum, the three-dimensional spectrum takes the form of Kolmogorov [3]

$$E(\kappa) = C\epsilon^{2/3}\kappa^{-5/3} \tag{8}$$

where C is the Kolmogorov constant ($C \approx 1.5$ if isotropy is assumed). It is demonstrated that the mixing transition, which

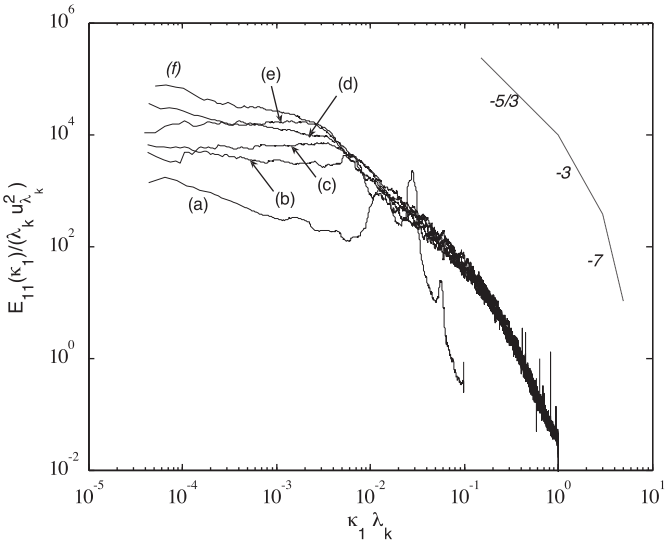

Fig. 15. Velocity spectra of u at $r/D=0$ and $Re_D = 30,000$. (a) $x/D=1$, (b) $x/D=3$, (c) $x/D=5$, (d) $x/D=10$, (e) $x/D=15$, (f) $x/D=20$. Reprinted with permission, from [83]; copyright © 2009, American Institute of Physics.

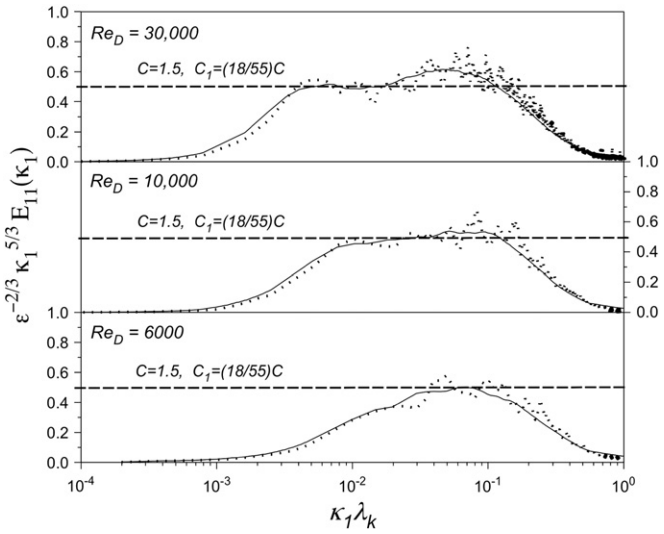

Fig. 16. Compensated velocity spectra of u at $r/D=0$ and $x/D=10$. Reprinted with permission, from [83]; copyright © 2009, American Institute of Physics.

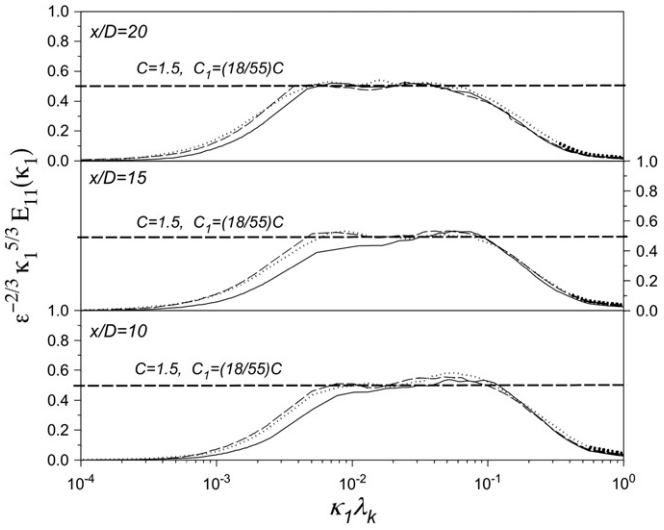

Fig. 17. Compensated velocity spectra of u at various radial positions and $Re_D = 10,000$. Solid line: r_1; discontinuous line: $r_{3/4}$; dotted line: $r_{1/2}$. Reprinted with permission, from [83]; copyright © 2009, American Institute of Physics.

occurs within the range $10,000 \leq Re_D \leq 30,000$, displays a different spectral energy content. The inertial sub-range is certainly apparent at $Re_D = 30,000$ but not at lower Reynolds numbers. The velocity spectra in the mixing layer are shown in Fig. 16). Citriniti and George [53] show that as the mixing layer is traversed radially, the peak in the spectra shifts to the low frequencies and the spectra display at least one full decade of $f^{-5/3}$ range, which denotes a high-Reynolds-number turbulent flow. The velocity spectra indicate that an increase in the source Reynolds number beyond $Re_D \gtrapprox 20,000$ and over approximately $x/D > 15$, the sub-range does not appear to be spatially sensitive; however, below $Re_D \approx 20,000$, spatial variability is observed (Figs. 17 and 18).

The effect of initial conditions on the velocity spectra was considered by Quinn [42], Mi et al. [41], and Xu and Antonia [52]. Quinn [42] found that the one-dimensional energy spectra and the distribution of the autocorrelation coefficients indicated the presence of large-scale coherent structures in both jets, with contraction and with sharp-edged orifice, and that these

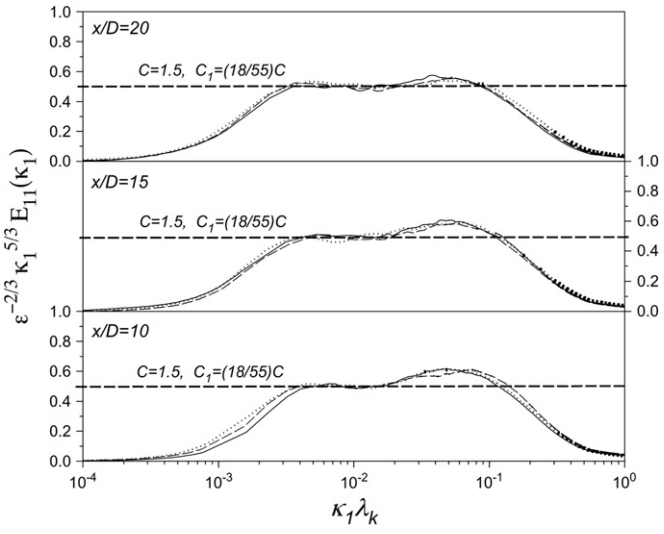

Fig. 18. Compensated velocity spectra of u at various radial positions and $Re_D = 30,000$. Solid line: r_1; discontinuous line: $r_{3/4}$; dotted line: $r_{1/2}$. Reprinted with permission, from [83]; copyright © 2009, American Institute of Physics.

structures are more 'energetic' in the sharp-edged orifice jet flow. Beyond the potential core, the one-dimensional energy spectra did not illustrate the effect of the initial condition; for both jets, the one-dimensional energy spectrum of the fluctuating streamwise velocity at $x/D=10$ was characteristic of fully turbulent flow.

The differences in the initial underlying flow structure of the three jets (contraction, pipe and orifice) were clear in the study of Mi et al. [41]. These differences were also reflected by the velocity power spectra within the shear layer. A broad peak in the velocity spectra was found for the jets from the contraction nozzle and the orifice plate. This reflects the quasi-periodic passage of coherent structures in the near field of the jets. The coherent structures occur generally at a higher frequency for the orifice jet than for the contoured-nozzle jet. Any large-scale structure, which may be present in the pipe jet, is aperiodic. Mi et al. [41] found that the large-scale coherent vortices that form in the shear layer of the orifice jet convect downstream at a higher speed than those for the contoured nozzle, presumably because the axial mean centreline velocity in the former exceeds that in the latter.

Xu and Antonia [52] indicated that in the shear layer, the spectra vary due to the differences of near-field structures in the pipe and contraction jets. At the same location, the pipe jet peak is always at a lower frequency than in the contraction jet. The lower frequency instability produced in the pipe jet results in longer wavelength structures, which develop and pair farther downstream. At the same distance from the virtual origin, the differences appear to diminish, although it is evident that the magnitudes of the peaks are quite different. The magnitude of the integral length scales associated with u-component is larger for the pipe jet than the contraction jet, whereas the magnitude of the integral length scales associated with v-component is smaller for the pipe jet. Measurement of the integral scales suggests a larger degree of anisotropy for the contraction jet. In the far field, the distributions of the axial and radial autocorrelation functions are nearly similar in both flows.

To close out this section, we may ask: why are spectra useful? A simple answer could be that it is helpful to identify the peaks that are typically associated with vortex shedding. Compensated spectra precipitate identification of the inertial subrange. Perhaps it is not the spectra per se that are important, rather it is the amalgamation of the contributions to them (that is, the energy content) by the myriad length scales. And, these are inherently

and inextricably linked to turbulence structures, to which we now direct our attention.

4.6. Coherent structures

Up to now, our review has focussed on investigations and reports that were based on statistical measures of the velocity fields of turbulent jets. This is not, however, the limit of fluid dynamicists' ability to understand jet flows; initially developed over 35 years ago, approaches based on 'coherent structures' are continually refined as we advance our ability to interpret flows. The overwhelming majority of studies of coherent structures were, in the early days, based on flow visualisations rather than quantitative data [80,90]. And so, we then benefited only from qualitative interpretations of organised motion that, unfortunately, suffer the bias inherent in an artist's perspective—an art admirer's interpretation of Salvador Dali's *Swans Reflecting Elephants* aptly demonstrates the rendered variability that fluid dynamicists generate when analysing (contemplating?) turbulent structures. In order to overcome this challenge, researchers continue to invent new quantitative interpretative techniques to better study the motion of coherent structures, their configurations, and their dynamical significance. Such improvements, having been recently accelerated, refine research outcomes in turbulence in general and with free turbulent flows in particular.

4.6.1. The basis of structures

Consider the following description of the formation of overall structure in round jets, as offered by List [91]; in just a few lines, List offers a description that remains true today, and that outlines the eminent research in turbulence structures up to the year 1982:

> The basic sequence for axisymmetric jets seems to be as follows: In the immediate neighbourhood of the orifice, the high-speed jet flow causes a laminar shear layer to be produced. The shear layer is unstable and grows very rapidly, forming ring vortices that carry turbulent jet fluid into the irrotational ambient fluid, and irrotational ambient fluid into the jet, as shown clearly by Crow and Champagne [64] and Becker and Massaro [90] (Fig. 19).
>
> The motion induced in the fluid by each vortex affects other vortices in such a way that adjacent vortices pair off, as discovered by Wehrmann and Wille [92] and shown in the photograph by Freymuth [93] (Fig. 20). The vortex motion develops a secondary circumferential instability that causes each vortex to break up, as discovered by Schneider [94] and Yule [95] and shown in Fig. 21. The situation is even more complicated in some cases by the presence and growth of helical waves that develop into helical vortices. These have been observed by Brown [96], Wehrmann and Wille [92], Plaschko [97], and Freeman and Tavlarides [98,91].

Following this sequence of events, the flow then becomes turbulent and the jet begins to spread outwards by engulfing ambient fluid. Within about 40*D* from the orifice, the jet becomes fully turbulent.

Consider, also, Robinson's definition of 'coherent structure:'

> A coherent motion is defined as a three-dimensional region of the flow over which at least one fundamental flow variable (velocity component, density, temperature, et cetera) exhibits significant correlation with itself or with another variable over a range of space and/or time that is significantly larger than the smallest local scales of the flow [99].

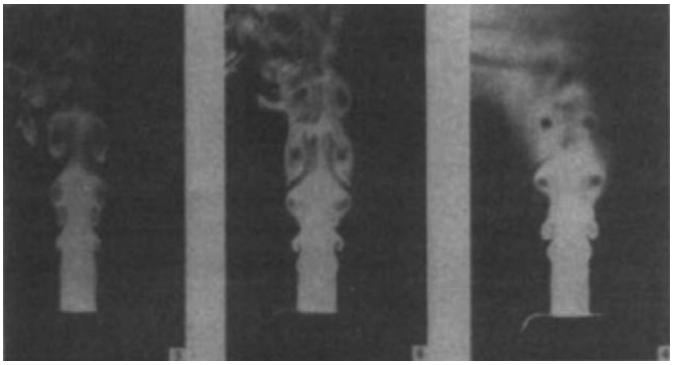

Fig. 19. Illustration of ring vortex production and fusion in a turbulent jet. Reproduced with permission, from [90]; copyright © 2006, Cambridge Journals.

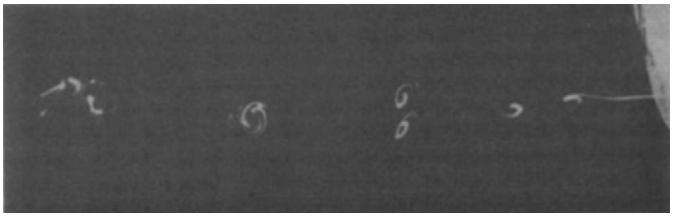

Fig. 20. Vortex pairing in a turbulent jet shear layer. Reproduced with permission, from [93]; copyright © 2006, Cambridge Journals.

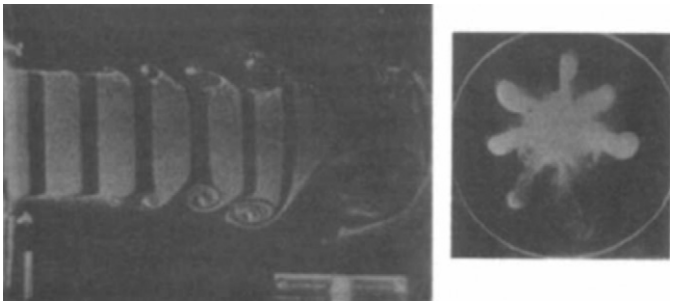

Fig. 21. Instability of ring vortices. Reproduced with permission, from [95]; copyright © 2006, Cambridge Journals.

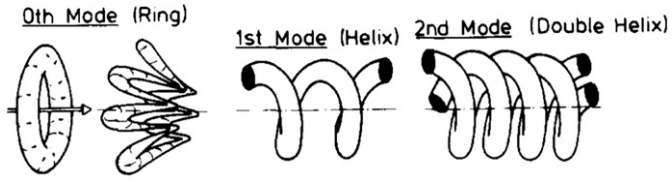

Fig. 22. Dominant vertical and helical modes in axisymmetric jet flow, basic structural modules. Reprinted from [100]; copyright © 1988 Pergamon Press plc., with permission from Elsevier.

Or, consider what was found in experimental studies by Crow and Champagne [64]; they established that the vorticity layer leaving the nozzle of the jet becomes unstable and forms Kelvin–Helmholtz waves which then roll up into vortex rings that are carried downstream to become three-dimensional and eventually break down. In addition to vortex rings, there is significant evidence of streamwise structures found both near the vortex cores and in the regions between successive vortex cores in the shear layer (braids) [95]. The evolution of streamwise vorticity in the braid region is due to the role of shearing forces that act perpendicular to the jet axis.

To clarify 'structures,' Fiedler [100] argued, in his review on the role of coherent structures in turbulent flows, that one or more dominant patterns can usually be recognised in a flow, and that these could be termed preferred modes which represent the most frequently occurring structures. In axisymmetric flows there are three equally distributed preferred modes; these are the ring, the single helix, and the double helix, as sketched in Fig. 22. In a further attempt to account for the role of structures in flows, Mungal and Hollingsworth [101] showed that the progression of organised structures through the jet is similar to that observed at lower Reynolds numbers. They concluded that the organisation of structures is associated with inviscid instability mechanisms that are independent of Reynolds number, and that large-scale organisation is an integral part of the evolution of the jet flow rather than a remnant of transitional behaviour.

It is quite clear that many different definitions for 'coherent structure' can be found in the literature [102,100]. Some images of coherent structures in round free jets are published in black and white in *An Album of Fluid Motion* by Milton van Dyke [103], and others. Consequently, the development of quantitative techniques such as particle image velocimetry (PIV), and the more recent advent of both tomographic (that is, volumetric) and time resolved PIV are exciting additions to the arsenal of the experimentalist.

The discovery of large-scale, quasi-deterministic coherent structures in flows which were previously considered chaotic is very exciting—it signals that the evolution of the structures and of the flows might be mathematically tractable [102]. The key feature is that they are vortical; that is, there is an instantaneously phase-correlated vorticity field underlying the random vorticity field that constitutes turbulence. Accordingly, understanding vortex interactions is crucial to understanding basic turbulence phenomena such as transport, mixing, turbulence production, and generation of aerodynamic noise [102].

4.6.2. Interactions of structures, vortex behaviour

The large-scale organisation in the transition region of the jet is due to the initial instability of the laminar shear layer near the nozzle. This instability is well understood from both experimental evidence and analytical analyses; according to Yule, [95], structures that form in the shear layer of the nozzle evolve downstream and then form periodic, circumferentially coherent fluid entities in the shear layer. The author concluded that, except at the lowest Reynolds numbers considered, this mechanism resembled the rolling-up of the laminar shear layer as it formed a period street of vortex rings [95].

Through flow visualisations, hot-wire anemometry measurements, and conditional sampling, Yule [95] investigated transitional and turbulent flows in the mixing layer region of a round free jet and characterised the transition region as the growth of three-dimensional flow caused by wave instability of vortex rings. In this growth, distorted vortices merge to produce larger eddies that remain coherent at least as far as the end of the potential core region of the jet. Whereas vortices are clearly arranged and easily visualised in the transition region, large structures in the fully developed turbulent regions are stronger but less evidently visualised. Yule showed that streets of vortex rings, with fully developed wave deformations of their viscous cores, entangle among each other in the transition to turbulence [95].

The breakdown of the jet and planar shear layers has been broadly investigated by Ho and Huerre [104], and by Huerre and Monkewitz [105,106]. Fiedler provided a good summary of these findings, as follows:

> A flow is considered absolutely unstable if the group velocity of an unstable mode is equal to zero. In this case the amplitude of a given perturbation grows with time at a fixed x-position in the flow. ... for convectively unstable flows all perturbation frequencies have positive group velocities. Thus, at a given $x \geq x_p$, where x_p defines the geometrical position at which the perturbation is introduced, the perturbation wave will reach a finite amplitude for a finite time only ... introducing a distinction between local and global instability: local instability denotes the situation of instability of a local velocity profile (being usually a function of x), while in global instability the entire flow field is concerned [2].

The 'modes' referred to above are those typically associated with Fourier decomposition of the signal, see for example [104] and references found therein. And, recall the earlier reference to 'modes' in Section 4.3.

Hussain and Zaman [107] re-iterate experimental evidence that a preferred frequency at which an axisymmetric disturbance is maximally amplified in the jet column in order to justify their experimental research by hot-wire measurements for the preferred modes of an axisymmetric free jet in the region $x/D \leq 14$ for $25,000 \leq Re_D \leq 110,000$. The jet 'column' mode was first identified by Crow and Champagne, [64]; a nice feature of this mode is its lack of vortex pairing. Hussain and Zaman wrote:

> The structure shape and size they [Crow and Champagne] found agree closely with those inferred from the average streamline pattern of the natural structure educed by Yule [95].

However, not even preferred mode excitation can sustain the organised large-scale coherent structures beyond the potential core (beyond $x/D \approx 8$). It was dawning upon researchers investigating turbulence structures that even the 'background turbulence' is organised by coherent motions; as a result, the maximum decay rate of coherent vorticity occurs at the structure centres—these are also the saddle points of the background turbulence Reynolds-stress distributions. In addition, the structure centres were also discovered to be the locations of peak phase-average turbulence intensities [107]. Hussain and Zaman [107] claim that the characteristic length scale of the mode is the jet diameter, not the width of the exit shear layer. It was also found that while the preferred-modes of coherent structures are independent of the state (laminar or turbulent) of the initial boundary layer, the size and orientation of the structures are Reynolds number dependent—with increasing Reynolds number, structures decrease in streamwise length, increase in radial width, and become more energetic and more efficient in production of Reynolds stress [64,107].

Flow visualisation experiments using laser induced fluorescence (LIF) in high-Reynolds-number turbulent jets were performed by Hussain and Clark [107]. From their observations it was suggested that at high Reynolds numbers the characteristics of coherent structures cannot be inferred from low Reynolds number observations—this is true even though coherent structures are inherent to all turbulent shear flows [107]. This substantiates the notion of a mixing transition. With increasing Reynolds number, coherent structures appear to be less frequent and more complex. Coherent structures are likely to be more dominant at higher Reynolds numbers, even though they occur less frequently; furthermore, the preferred mode coherent structure of an axisymmetric mixing layer becomes more rounded in cross section, and becomes responsible for larger coherent Reynolds stress (i.e. transport of momentum) with increasing Reynolds number [107].

At Reynolds numbers $Re_D \approx 2500$ and $Re_D \approx 10,000$, Dimotakis et al. [80] showed the presence of large-scale vortical structures in the far field that appear to be usually axisymmetric or helical. These large structures not only dominate the flow dynamics in

the transition region (as previously documented), but also in the far field—this discovery is one of the earliest confirmations of organised helical and axisymmetric motion in the far field. It is difficult to discern these motions because the energy content of coherent motion in jets is low (about 10% of the total turbulent kinetic energy) compared to mixing layers (about 20%) [100]. Dimotakis' et al. [80] conclusion that large scale vortical structures dominate the dynamics throughout the flow field of a turbulent jet was based on a visual observation of both zig–zag and symmetric flow patterns. Keep in mind that such observations are like an artist's interpretation; Hama [108], among others, asserts that interpretation of smoke pictures is fallible. From flow visualisations, we only know for certain that the structures in a turbulent flow have differences in their geometrical and dynamical features which may be characterised by shape, size, orientation, strength, lifetime, convection velocity, and so on, and so forth.

Further work on coherent structure eduction using controlled excitation in combination with conditional sampling techniques is described and reviewed in Hussain [102] in which the existence of azimuthal vortex pairing is confirmed while detailed topographical measurements of the coherent rings are produced. Vortex pairing based on Strouhal number was found to occur in two ways: the jet column, and the shear layer.

It had been assumed that structures are responsible for the finite correlation at large scales (i.e. larger than the integral scale), and to carry 10–20% of the total turbulent energy. Large structures were viewed as passive contributors to the flow dynamics. Glauser was the first to quantify these large coherent structures by implementing the proper orthogonal decomposition (POD) technique in the near field of an axisymmetric jet; through this effort, a rapid energy convergence with mode number was demonstrated [109–111]. The first POD mode was found to contain nearly 40% of the turbulent energy, whereas, the first three POD modes captured nearly all the resolved turbulent kinetic energy [111]. Glauser and George built upon this work by adding a second rake of seven straight-wires to obtain, at the same streamwise position, cross-spectra for both the radial and azimuthal probe separations [110]. Recently, to determine whether the axisymmetric mode is dominant, Iqbal and Thomas interrogated the energy of the first azimuthal POD mode $m=0$, relative to the energy contained in all other azimuthal modes, and found the energy ratio to be about 0.23; this indicates that a few higher azimuthal modes should be included in the definition of coherent structure [57]. The conundrum of the definition of coherent structure continues.

Tso and Hussain [112] conducted an experiment at $Re_D = 69,000$ using a radially aligned linear rake of cross-wires to study the occurrence, configuration, and dynamics of large-scale coherent vortical motions in the fully developed region of a turbulent axisymmetric jet. Vorticity signals from a spatial grid were used to detect and sample large scale vortical structures to determine their configuration and dynamics by aligning and ensemble averaging successive realisations of the signals. While structures with axisymmetric, helical and double helical configurations were all educed, it was found that helical structures were dominant. Their radial outward movement with downstream advection, concurrent with ejection of local turbulent fluid and antecedent to mixed turbulent/ambient fluid entrapment, seems to be the significant manner by which the jet spreads; this is achieved by intense small scale turbulence mixing in the downstream side of the structures [112].

Kirby et al. [113] were the first to use a snapshot POD method to create an ensemble of conditionally sampled flow realisations produced by a two-dimensional LES of an axisymmetric jet at $x/D=6$. While their results were interesting, the important outcome from the study was the use of 'snapshots' to decrease the computational time required to obtain the empirical eigenfunctions. The snapshot POD is now widely applied to both computational and experimental data sets.

Dahm and Dimotakis [114] applied laser induced fluorescence (LIF) visualisation between $0 \le x/D \le 350$ of an axisymmetric turbulent jet. They noted:

> The organisation in the jet far field appears to be both topologically and dynamically more complex than that in turbulent shear layers, and may be a consequence of the fact that the jet is simultaneously unstable both to axisymmetric and helical modes, and appears to alternate between these two [114].

The instantaneous concentration field was ordered in the form of arrowhead-shaped structures, with marginal variation of concentration within these structures. Agrawal and Prasad [115] found similar structures after their data were low-pass filtered ($110 \le x/D \le 175$); attention will be turned to this paper a little later.

The role of streamwise vortex structure evolution in the near field ($x/D < 10$) was examined by Liepmann and Gharib [82] who used LIF to show that entrainment is determined primarily by streamwise vorticity beyond the end of the potential core regime. The initial Kelvin–Helmholtz instabilities develop, as does the subsequent vortex rollup; these, together, lead to the formation of a series of azimuthally unstable vortex rings that grow as they move downstream by entraining ambient fluid, as seen in Fig. 23. Interestingly, a short time later, Citriniti and George concluded:

> Results of the velocity reconstruction using the POD provide evidence for azimuthally coherent structures that exist near the potential core. In addition to the azimuthal structures near the potential core, evidence is also found for the presence of counter-rotating, streamwise vortex pairs (or ribs) in the region between successive azimuthally coherent structures

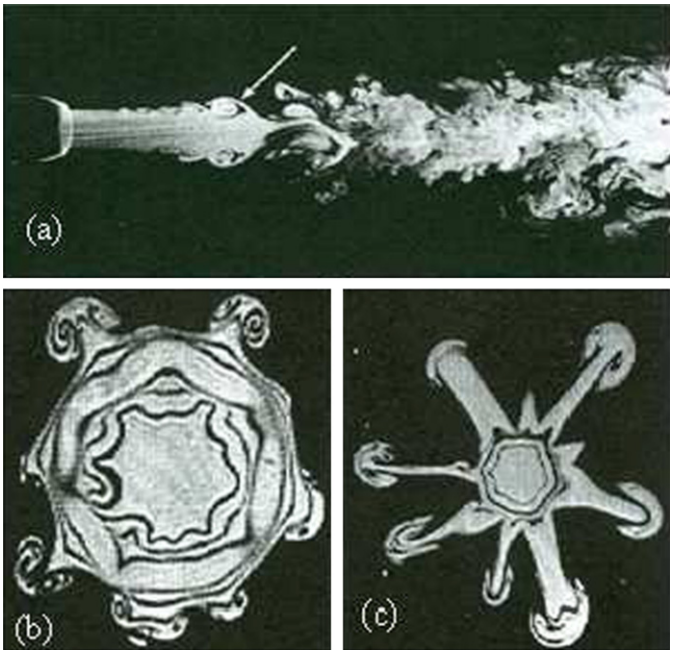

Fig. 23. Round jet flow visualisation. LIF side-view, $Re_D \approx 5500$; the arrow indicates a streamwise structure at $x/D=3.5$. LIF cross-sections. Ring at $x/D=3.5$ and (right) braid at $x/D=3.5$. Reproduced with permission, from [82]; copyright © 1992, Cambridge Journals.

as well as coexisting for short periods with them. The large-scale structure cycle, which includes the appearance of the ring structure, the advection of fluid by the ribs in the braid region and their advection toward the outside of the layer by a following ring structure, repeats approximately every one integral time scale. One surprising result was that the most spatially correlated structure in the flow, the coherent ring near the potential core which ejects fluid in the streamwise direction in a volcano-like eruption, is also the one with the shortest time scale [53].

After the potential core region, the centreline velocity begins to decay. These events reduce the velocity difference between the ambient fluid and high speed core of the jet, and attenuate the shear that supports the vortical rings of the jet. In jets, this attenuation of shear activates the interactions and competition between the elements of azimuthal and streamwise vorticity which, consequently, causes abrupt decay of the vortex rings into smaller structures. Small perturbations grow in the highly strained region between pairs of vortex rings to form secondary instabilities which again produce streamwise vortex pairs—these appear as mushroom shaped structures surrounding the rings. These may extend outward from the centre of the jet, but always remain contiguous with the central flow. The extent of this spread of the jet into ambient fluid was determined by Cenedese et al. [116]; from both LDA and PIV measurements of jets over the range $2000 \leq Re_D \leq 25,000$, iso-velocity contours of streamwise and transverse velocity showed that jets spread into ambient fluid with an opening angle between 20° and 35°.

The myriad features of vortex rings are shown in Fig. 23. Additional visualisations, also from Liepmann and Gharib [82] show that initial instabilities grow in the braid region and are subsequently attenuated by the primary ring. As the flow develops, the rings become unstable relative to each other and tilt so that they are no longer normal to the axial flow direction. In a round jet, pairing causes both contraction and expansion of the primary vertical rings; this might enhance the evolution of the secondary, three-dimensional structures. Citriniti and George [53] and McIlwain and Pollard [54] found, like Liepmann and Gharib [82], that the entrainment in the near field of a jet is dominated by braid structures.

Streamwise vortices, visualised in an $Re_D = 78,000$ jet by Paschereit et al. [117] using both schlieren and dye photography, were found to represent secondary instabilities inherent to the perturbed shear layer that surrounds the jet column. Furthermore, the existence of helical and axisymmetric modes in the far field of an $Re_D = 5000$ natural, circularly and axially forced jet were identified by Yoda et al. [46] who found that both helical and axisymmetric modes exist in the far field of the natural jet, but that the flow tends to shift between the two modes.

Coherent streamwise structures were studied for two Reynolds numbers, $Re_D = 5500$ and $Re_D = 16,000$ by Weisgraber and Liepmann [118] through PIV measurements in the region $15 \leq x/D \leq 30$. They described their work:

The study consisted of instantaneous snapshots of the velocity and vorticity fields as well as measurements of velocity correlations up to third order. In this regime, the Reynolds number had a significant effect on both the instantaneous flow structure and the profiles of mean velocity across the jet. Coherent streamwise structures were present in the jet core for the lower Reynolds number. Additional structures whose evolution was governed by time scales two orders of magnitude larger than the convective scale inside the jet were observed in the entrainment field [118].

Pockets of vorticity, associated with what are now known to be either ring-like braids or simple 'vortical' structures, were found to manifest within mean and instantaneous vorticity in both azimuthal and streamwise directions. It was observed that structures educed from the vorticity plots display increased finer scales with increasing Reynolds number (i.e. the aforementioned pockets); however, evolution of the flow as a function of Reynolds number that is below the 'mixing transition' (see Dimotakis [59]) is difficult to glean from only two sets of data.

Experimental results of Drobniak et al. [119] identified some typical features of heat transport in the very near field of a round free jet characterised by the presence of organised motion. Their experiments were performed by forcing the jet to be in the 'column-mode' and by using a triple hot-wire for velocity measurements. Four-wire probes are now more widely available and have been used in jets; heed, in particular, the advice that, while the use of four-wire probes may eliminate the need to correct for off-axis velocities (and simplify experimental interpretation of three-dimensional flow data), the acceptance domain of four-wire probes may not be sufficiently large to achieve accurate measurements in high turbulence intensity flows [120]. Drobniak et al. found that substantial intensification of the radial heat transport results from the mutual phase relationships between oscillatory and random components of velocity and temperature; as a result a much wider temperature spread of the temperature field, as compared to the velocity field, may be observed as a characteristic feature of the flow. Heat transfer processes come about by random turbulence generated by the action of coherent motion [119]. It is perhaps baffling that coherent motions may generate random turbulence. This is, again, the issue of perception that we liken to the interpretation of Salvador Dali's art.

Recently, various statistical analysis tools – conditional sampling methods, variable interval time average (VITA) methods, and quadrant methods, among others – have emerged to detect and characterise coherent structure motions (see Robinson [99] for a taxonomy applied to a boundary layer). As an aside, Sullivan and Pollard [121] compared different analytical methods for the identification of coherent structures from multipoint measurements made in a three-dimensional wall jet. They used POD, linear stochastic estimation (LSE), Gram–Charlier estimation (GCE) and wavelet decomposition (WD). The comparison of both POD and LSE results shows that each captures essentially the same information. The GCE is used to develop a spatially dense mapping of the instantaneous flow. Wavelet decomposition was found to offer a more general method for investigating a flow field. These methods were applied and the resulting information analysed to educe structure. Bonnet et al. [122] also compared different techniques: conditional sampling, wavelets, pattern recognition analysis, POD, LSE, topological concept-based methods, and full-field methods. Good quantitative and qualitative agreement between the different methods was observed.

Since each sampling criterion extracts a different feature of the flow, some confusion has arisen from comparisons between the results obtained from different techniques. More sophisticated statistical techniques employed to educe the structure of organised turbulence motions include POD and stochastic estimation of the single-point and two-point correlation tensors. Useful multipoint measurement techniques to study the coherent structures are reviewed in Glauser and George [123]. Citriniti and George [53] complemented the work of Glauser [109] to examine the dynamics of the axisymmetric jet shear layer. They used 138 synchronised channels of hot-wire anemometry, for $Re_D = 80,000$ and at $x/D = 3$. They applied POD to reconstruct the global velocity field and obtained the local temporal dynamics of the flow field. It was shown that only five azimuthal modes ($m = 0, 3, 4, 5, 6$) are required to faithfully represent the local

dynamics of the large-scale structure. From their data, they found that azimuthally coherent structures (rings or volcano-like) exist near the potential core. These rings eject high-streamwise-momentum fluid through their cores; this event creates the aforementioned bursting event. In addition to the azimuthal structures, they found evidence for the presence of counter-rotating streamwise vortex pairs (or ribs) in the region between successive azimuthally coherent structures. The ribs are strengthened in the high-strain region between successive rings. That is, the induced velocity field between successive rings creates a high-strain field that seems to play an important role in the evolution of ribs. The large-scale structure cycle, which includes the appearance of the ring structure, the advection of fluid by the ribs in the braid region and their advection toward the outside of the layer by a following ring structure, repeats approximately every one integral time scale. Citriniti and George [53] discovered the important result that the most spatially correlated structure in the flow, the coherent ring near the potential core which ejects fluid in the streamwise direction in a volcano-like eruption, is also the one with the shortest time scale.

Arndt et al. [124] measured the pressure signal at the outer edge of a jet mixing layer to study the large-scale structure of the turbulent flow. They demonstrated that the fluctuating pressure signal can be used to deduce large-scale flow structures embedded within the jet. To deduce the streamwise structures, they used POD on the pressure signal obtained from multiple microphones positioned at the edge of the jet and distributed along the streamwise direction. The energy extracted for the pressure fluctuations is associated with each azimuthal mode. The axisymmetric mode (mode 0) contained 50% of the total energy, the helix mode (mode 1) contained 23%, the mode 2 contained 14%, and mode 3 contained only 5% of the energy.

> The POD streamwise eigenfunctions show that the structure associated with any frequency-azimuthal mode number combination displays the general characteristics of amplification-saturation-decay of an instability wave, all within about three wavelengths. High-frequency components saturate early in x [*that is, in the axial direction, au.*] and low-frequency components saturate further downstream, indicative of the inhomogeneous character of the flow in the streamwise direction. Application of the POD technique allows the phase velocity to be determined taking into account the inhomogeneity of the flow in the streamwise direction. The phase velocity of each instability wave (POD eigenvector) is constant and equal to $0.58\,U_j$, indicating that the jet structure is non-dispersive. Using the shot-noise decomposition, a characteristic event is constructed. This event is found to contain evidence of both pairings and triplings of vortex structures. The tripling results in a rapid increase in the first asymmetric ($m=1$) component. On average, pairing occurs once every four U_j/D while tripling occurs once every 13 U_j/D [124].

They showed that the vortex pairing does not occur in a repeatable fashion at a specific downstream location but is random in both time and space. Glauser's group at Syracuse University continue to explore the use of noise for control of mildly compressible jets, see [125].

In addition to the work of Paschereit et al. [117] on the formation streamwise braid structures between the ring structures, McIlwain and Pollard [54] used an LES with a dynamic Smagorinsky subgrid scale model to investigate the near fields of turbulent round free jets in order to understand the temporal and spatial interaction between the rings and braids. They showed two regions that correspond to a ring-shaped structure at $x/D=2$. The ring is slightly distorted in the axial direction despite the perfectly symmetric forcing at the jet nozzle, indicating the presence of a negative helical mode $m=-1$. The formation, convection, and interaction of the rings and the braid were illustrated from several snapshots of the instantaneous vorticity. Further reference to these simulations will be made below.

Mi et al. [41] showed that the nozzle shape leads to clear differences in the initial underlying flow structure of the three jets. Well defined coherent vortical structures are visually evident in the near field in the jet from the contraction nozzle. The same coherent structures are also evident along the potential core of the orifice jet, although not as well defined as those from the contraction nozzle. In contrast, there are few coherent structures discernible in the near-field region of the pipe jet.

Romano [45] investigated the near flow field ($0 \le x/D \le 5$) of an axially symmetric water jet over $1000 \le Re_D \le 10,000$ using LIF, LDA, and particle tracking velocimetry (PTV) with a focus on rigid or free boundary nozzle outlet effects (no-slip or free-slip conditions, the axisymmetric nozzle exit plane is either flush with a back wall or is positioned upstream with the nozzle intruding into the receiving tank). The velocity profiles are therefore the same at the exit of the nozzle in both cases; both spanwise and streamwise vortices on the longitudinal plane and on cross-sections were observed. It was found that, on average, for the free-slip jet (where the nozzle extended inside the tank) these structures developed more gradually and closer to the nozzle than for the no-slip jet (where the nozzle is placed flush with the wall). The large structures grow and break up closer to the nozzle in the case of the free-slip jet which increases the mixing compared to the no-slip jet.

Ganapathisubramani et al. [126] used stereo PIV techniques to investigate a round air jet at $Re_D = 19,000$ to understand the characteristics of all three velocity components in the developing shear layer, and to study the effect of axial distance on the evolution of three-dimensionality. To quantify coherent structures, they used both swirl strength (λ_i) and the Q-criterion [127]. They argue that the Q-criterion is a more appropriate index than vorticity since it represents only the intensity of the rotating fluid motion and does not involve the contribution of the shear transformation; this will be considered again a little further in the paper, with reference to [128]. Ganapathisubramani et al. [126] also showed that both vortex cores and braids are three-dimensional, are formed as early as $x/D \approx 0.5$, evolve and pair up to form larger-scale downstream structures, and are correlated to azimuthal velocity and its derivatives. The braids contain streamwise vortex tubes aligned with the flow direction while the cores may possess significant azimuthal velocity. The initial azimuthal perturbations are typically associated with straining regions immediately upstream of the first vortex ring that formed at the downstream location of $x/D=0.5$.

Producing results consistent with those of Yoda et al. [46] and Tso and Hussain [112], Agrawal and Prasad [129] studied large vortices that occur in the axial plane of a self-similar axisymmetric turbulent jet by spatially filtering PIV data at $Re_D = 3000$. Large vortices tend to organise themselves in preferred modes; evidence of ring and helical modes were revealed by Galilean transformation of the low-pass filtered field (i.e. by subtracting 15% of the mean centreline velocity). While the helical mode (see Fiedler [100]) is more frequent, both modes seem to occur prominently in jets; overall diameters for both modes are comparable to the local half-jet width. The double helical mode, however, is more difficult to observe, and was not discerned from their data set. Mode types aside, large entrainment of ambient fluid and jet meander were found to be the primary features associated with the production of large scale vortices. Being sparsely populated with weak vortices, regions at large $r/r_{1/2}$ tend to have a low overall vorticity; this corresponds to other

findings of Agrawal and Prasad [115,130] that vorticity, which is maximal at the vortex core, decreases monotonically with increasing radial co-ordinate. While, according to their results, the centre of a larger vortex will spin faster than that of a smaller (in an ensemble averaged sense) and the average energy of vortices increases with the square of vortex radius, this trend reverses at the core edge to give the expected result. Agrawal [131] has recently determined an 'analytical solution for vorticity, tangential velocity, circulation and pressure inside vortex cores in turbulent flows'. His analysis 'suggests a linear decrease in vorticity and polynomial variation for other quantities with distance from the vortex centre' [131].

In the near field ($2 \le x/D \le 6$) Jung et al. [132] and in the far field ($20 \le x/D \le 69$) Gamard et al. [133,134] used the same hot-wire array as Citriniti and George [53] to investigate the evolution of modal energy. Their experiments showed that the POD eigenspectra varied significantly in the downstream direction and were nearly independent of Reynolds number. They demonstrated a progressive shift of the dominant azimuthal mode from $m=0$ at $x/D=3$ to azimuthal mode $m=2$ by $x/D=6$. In the far field, the azimuthal mode $m=2$ continues to dominate the flow. Gamard et al. [133,134] measured, on different planes in the fully developed region of the round jet, the two-point velocity correlations with separation distances in the radial and azimuthal direction. They showed that these correlations collapse when they were scaled correctly. In these investigations, the three-dimensional streamwise velocity field was shown to evolve from 'volcano-type' to 'propeller-like' patterns with downstream position; in the near field, structures were seen to have strong dependence on streamwise position.

Suto et al. [135,136] used large eddy and direct numerical simulation, respectively, to uncover the coherent structures of the developed jet. They used top-hat and 'hyperbolic' inlet mean velocity profiles, but did not note any substantial difference in the structures when well removed from the nozzle exit plane. They proposed a conceptual model of a hairpin-shaped vortex and validated it by two-point correlations and probability density function (PDF) analysis for vortex alignment. They observed pairs of vortices in the jet outer layer and streamwise vortices in the jet central region, the latter being roughly half the jet half width in size. The hairpin-shaped vortices formed in the background shear of the mean flow 'stand' with 'legs' inclined at roughly 45° to the mean flow direction; these vortices were offered by Suto et al. [136] as being among the universal structures in turbulent shear flows.

Using a stereo-PIV system, Matsuda and Sakakibara [137] measured turbulent vortical structures at $20 < x/D < 50$ over a Reynolds number range $1500 \le Re_D \le 5000$. Vortical structures were visualised by iso-surfaces of swirl strength, λ_i, which was defined using a local vortex diameter or length scale divided by a convective velocity obtained assuming Taylor's frozen eddy hypothesis. This provides a representation of the intensity of the rotating fluid motion only, but does not include contributions made by shearing transformations; it corresponds physically to the angular velocity of the swirling motion, and mathematically to the imaginary part of the complex eigenvalue pair of the local velocity gradient tensor. The existence of a group of hairpin vortex structures was evident around the rim of the shear layer. The centre of curvature of the heads of these hairpin vortices was near $r/r_{1/2} \approx 1.5$, and their legs were spaced azimuthally by about $0.9\, r_{1/2}$; typically, leg spacing was independent of Re_D. Overall, the arrangement of organised structures is axisymmetric in the near field, but less so in the far field.

Over approximately the same Reynolds number range ($177 \le Re_D \le 5142$), Kwon and Seo [138] also used PIV to study Reynolds number effects. A series of figures analogous to those in Dimotakis et al. [80] was presented to demonstrate the very low Reynolds number instability that was described by Crow and Champagne [64]; notwithstanding, the stated purpose of the study was to focus on characteristics of velocity and turbulence variation with Reynolds number. While Reynolds number dependence of several statistics was reported, physical explanations for the observed phenomena were not offered.

Bogey and Bailly [139] have performed LESs of turbulent jets and report Reynolds numbers effects on round jets in the region $0 \le x/D \le 20$. These were shown to have a significant effect on mean flow and turbulence statistics development in both the shear layer and the transitional region downstream of the potential core. With lower Reynolds numbers, higher turbulence intensities, larger integral scales and more rapid development were all observed. These simulations were conducted for $Re_D = 1700$; 2500, 5000; 10,000; and 400,000. Such Reynolds numbers are either below or far above the mixing transition range proposed in Dimotakis et al. [80] and Dimotakis [59]. This mixing transition that occurs at Re_D well above the laminar-to-turbulence transition for a round jet presents a subsequent and often well-defined additional transition in the flow—particularly with regards to the flow structures [83].

Shinneeb et al. [140,141] experimentally investigated vortical structures in the near-exit region of a round turbulent jet with $Re_D = 21,900$. The measurements were made using PIV; the data were analysed using POD to expose the main energy-containing structures. They used the vortex identification algorithm of Agrawal and Prasad [115] to identify the structures and quantify their size, position, circulation, and direction of rotation. Their data clearly showed the formation of alternating-direction toroid vortices which begin to be resolved at a streamwise location of one-half the jet exit diameter. Thereafter, the number of vortices decreased and their size and circulation increased as they convected downstream.

Iqbal and Thomas [57], by a vector implementation of the POD, experimentally characterised the time-averaged coherent structures in the near field of an axisymmetric turbulent jet at $Re_D = 380,000$ and $Ma=0.3$. The phase information required for a local reconstruction of the jet structures was obtained by projecting the POD eigenmodes onto instantaneous realisations of the flow at fixed streamwise locations. Their large structure topology showed that the helical large-scale structures dominate the coherent structures in the jet flow and that they persist or survive beyond the tip of the jet core. They showed that the dynamic behaviour of each component of the jet structure is local. From the governing equations for the two-point velocity correlations in the far field of the axisymmetric jet, Ewing et al. [85] showed that these equations can have equilibrium similarity solutions for jets with finite Reynolds number that retain a dependence on the growth rate of the jet. Starting from the two-point correlation, they claimed that the turbulent processes that produce and dissipate energy at different scales of motion, as well as transfer energy between the different scales of motion, are in equilibrium as the flow evolves downstream. Their results provided evidence that the two-point correlations are statistically homogeneous in the streamwise similarity coordinate.

The LES data of McIlwain and Pollard [54] for the near field of a round jet have been re-analyzed by Sheridan and Pollard [128]. These data, for $Re_D = 68,000$ and over $0 < x/D < 5$, have been subjected to interrogation using the Q-criterion [127], the negative second eigenvalue ($-\lambda_2$) criterion [142], helicity magnitude $v \bullet w$, palinstrophy $1/2|\nabla \times w|^2$, enstrophy $w^2 = 1/2|\Omega \bullet \Omega|$, and the Lamb vector $v \times w$. The educed structures, provided in Fig. 24, indicate that the near field of this jet displays structures that are nearly homologous.

The vorticity magnitude and enstrophy educe similar regions as the eigenvalue based techniques since they are directly

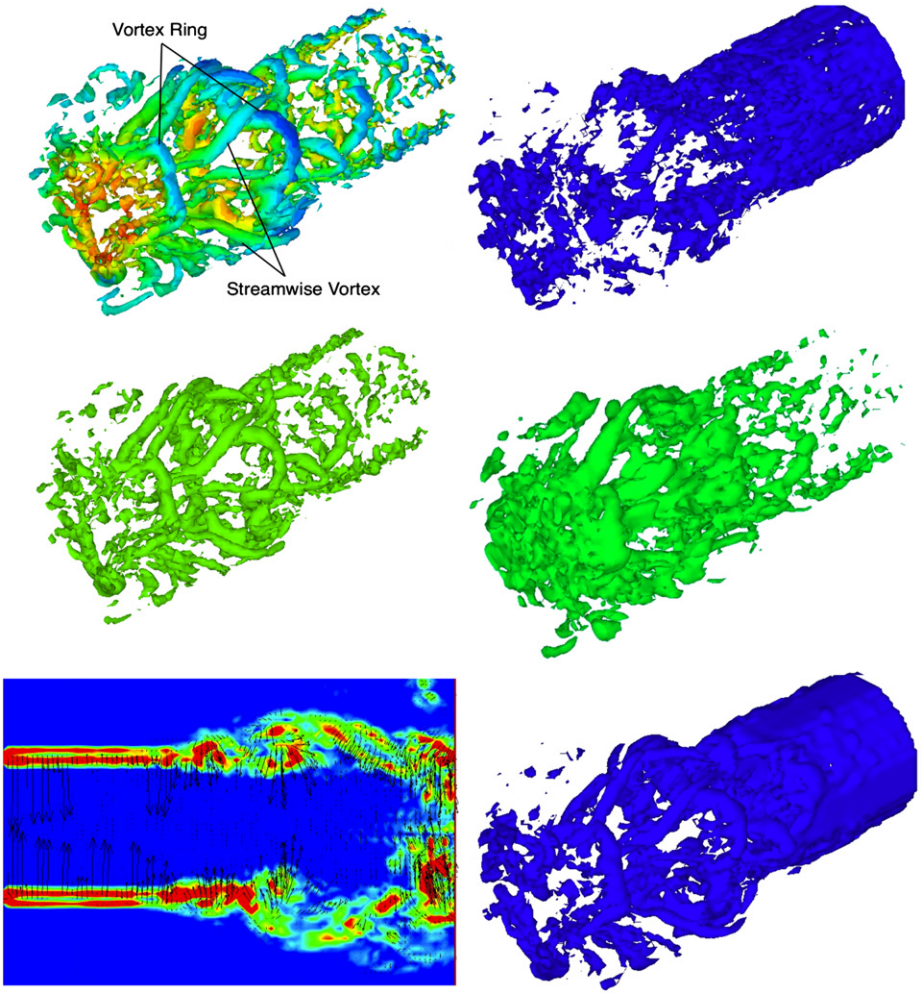

Fig. 24. Perspective views of structure from LES data using different vorticity-based methods, $0 < x/D < 5$. The enstrophy-Lamb vector composite locates vortex cores as the vector points outward from regions of high planar vorticity (red). Clockwise from upper left: Q-criterion coloured by axial velocity magnitude; palinstrophy; helicity; enstrophy; enstrophy and Lamb vectors; negative second eigenvalue. (For interpretation of the references to color in this figure legend, the reader is referred to the web version of this article.)

proportional to the vorticity in the flow. However, these techniques include much more noise, especially near the exit of the jet. The helicity results are harder to interpret since they represent the 'corkscrewing' of the flow—this is not as intuitive as the typical picture of vorticity. The educed region shows that the most highly corkscrewed type motion occurs near the tangle of streamwise vortices and vortex rings near the exit of the domain. It is expected that regions of higher helicity would correspond with streamwise vortices, since it is at these locations where the velocity and vorticity vectors would be similarly oriented. The results for the palinstrophy show that the locations where the magnitude of the curl of the vorticity is greatest are those at the exit of the jet, near the locations of the vortex rings, and at the exit of the domain. The low values of palinstrophy in the region where the streamwise vortices are dominant is due to the lack of rotation of the fluid in this region.

In order to use the Lamb vector to compare with the other visualisation techniques, a contour plot was made of the helicity, palinstrophy and enstrophy on the central plane of the jet with the Lamb vectors overlaid. These results show that the Lamb vectors are closely associated with regions of higher enstrophy, much more than regions of either helicity or palinstrophy (these are not shown). This is expected since enstrophy is so closely related to vorticity, and the Lamb vector points away maximally from regions of high planar vorticity. It can also be seen that the Lamb vector is a good indicator of the location of the vortex rings on this plane. For this slice of the domain, the cross-section of the vortex ring appears as a planar vortex, with the vorticity vector perpendicular to the plane and the velocity vectors circulating around it.

Clearly, the topic of 'Coherent Structures' in turbulent flows remains complex. Technological and analytical advances have provided new ways to interpret, that is to 'see,' the flow. However, evolution in our understanding of the flows has been tempered by the overwhelming wealth of knowledge afforded by the multitude of structure eduction techniques, with accompanying variations in interpretive practice. And so we remain, in a way, beset by the caprices of an art admirer—it is still very difficult to recount the big-picture 'story' of coherent structures in a turbulent round jet.

5. Looking to the future

The effect of the initial conditions on the development of flow from a jet is important to establish how rapidly the flow disentangles from conditions at the flow origin. Typically, three alternative types of nozzle have been commonly used: smoothly contracting nozzles, long pipes, and orifice plates. The exit velocity profile of a long pipe jet is non-uniform, and can be

described empirically by a power-law. The boundary layer is also in a fully turbulent state at the pipe exit and possesses a thicker initial shear layer and larger turbulence intensity than the contraction jet. The velocity profile and the near-field flow structure are more complex in the jet that issues from an orifice plate. The rate of mixing is higher in jets issuing from an orifice plate, while the pipe jet has the lowest rate. The measurements for the 'potential core lengths,' the mean streamwise velocity decay rates, the jet spreading rates, the mean static pressure recovery and the Reynolds normal and shear stresses show that mixing, which governs the evolution of the jet, is higher in the sharp-edged orifice jet than in the contraction nozzle jet. It has been established that the near-field differences are linked to significant differences in turbulence structure. Boersma et al. [67] found that (for low *Re*) when the initial velocity profile is similar to that for a fully developed pipe flow, the distance between the ring vortices is larger than in the contraction jet. In the velocity spectra, it was noted that the larger initial boundary layer thickness produces dimensionally lower frequency instabilities, which develop and pair at larger distances downstream. An increase in the initial boundary layer thickness of a round jet results in an increase in the streamwise location where the primary vortex structures roll up, and a corresponding increase in the length of the potential core, according to Russ and Strykowski [143].

For any given initial condition, statistical data are generally in good agreement between different investigations. Large scale coherent structures that are dominated by the helical mode are found in the far field, according to Tso and Hussain [112]. Whereas Yoda et al. [46,47] suggest that the far-field large scale structures are present continuously, switching between helical and axisymmetrical modes.

In George [4], two conjectures regarding the determination of the route by which a flow attains self similarity were put forth. The first states that a flow will always asymptotically reach a fully self-similar state if its governing conditions (equations of motion, boundary conditions, and initial conditions) so permit; what is required for such 'permission' is, as yet, uncertain. The second conjecture allows for partial and local self-similarity in cases where governing conditions do not admit to a fully self-similar solution. So, for a particular type of flow, there exists a multiplicity of self-similar states that are uniquely determined by initial conditions. These conclusions were drawn from a theoretical analysis of self-similarity, especially as pertaining to jets and wakes.

In a survey of published experimental data on jets and plumes, Carazzo et al. [77] use the equation for flux of mean kinetic energy defined by Priestley and Ball [144] to provide a quantitative investigation into the route to self-similarity. The results of Antonia and Zhao [72] indicated that, despite the quite different initial conditions, the two axisymmetric jets considered, contraction and pipe, reach the same state of self-similarity at approximately the same x/D. In their analysis, Carazzo et al. [77] showed that both jets and plumes displayed multiple states of partial and local self-similarity, as predicted in George [4]. In contrast, they concluded that global evolution of jets and plumes proceeds towards complete self-similarity via a universal route. In coming to these conclusions, Carazzo et al. [77] define an entrainment coefficient, αe, which is a function of Reynolds-averaged profiles that depend on velocity, buoyancy, and the turbulent stresses. The formulation of the entrainment coefficient permits a quantitative description (by proxy, through its terms) of the evolution of self-similarity.

Carazzo et al. [77] reported, however, that most of the studies upon which they based their conclusions were carried out with insufficiently large ranges of x/D to definitively test the hypothesis of self-similarity. It appears, furthermore, that the range of Reynolds numbers for each of the data sets could be too narrow (one spans $2460 \leq Re_D \leq 10,900$), especially in light of the mixing transition hypothesis [59].

By choosing the effective jet width, Δ, as a length scale – one that reflects the effect of the viscous layer at the orifice exit – Uddin and Pollard [43] propose that the role of inlet conditions on self-similarity (and the virtual origin) can be better understood. Their proposed hypothesis on the dependence of the virtual origin was tested against their LES data for $Re_D = 7,300$, as well as the high Reynolds number experimental data of Nickels and Perry [78], in order to validate it beyond the mixing transition. However, no data in the mixing transition range of Reynolds numbers were used.

As mentioned earlier, Dimotakis [59] proposed the existence of the mixing transition in which, among other things, the nature of the mixing of a scalar is observed to change dramatically near a critical Reynolds number. The fully-developed flow requires an outer-scale greater than 10,000 to 20,000 or a Taylor Reynolds number greater than 100 to 140. For shear layers, this transition is correlated with a transition to three-dimensionality; for round jets, being already three-dimensional, such a correlation is not possible. In his review, Dimotakis [59] relied upon scalar measurements and qualitative observations to identify the mixing transition in turbulent jets. As inspired by Dimotakis [59], further investigations into the mixing transition were conducted and reported by Fellouah et al. [84,83] to characterise and understand the concept of mixing transition in the round free jet. Their measurements of velocity spectra and calculations of the various micro-scales over a Reynolds number range that should include the mixing transition showed that, beyond the mixing transition of approx $Re_D = 20,000$, the energy of the large-scale turbulence proceeds directly to the dissipation range while the compensated velocity spectra are accompanied by the appearance of the inertial subrange.

Clearly, there remains discord regarding the role of initial conditions in the route to self-similarity. In light of the mixing transition hypothesis for jets (and recognising an apparent gap in the knowledge base) it would be useful to learn from the data sets of mean velocities and higher order moments in the near and intermediate fields of a round jet for a Reynolds number range that spans the mixing transition range; see Ball and Pollard [145] for a tabulated compendium of works.

From this review, we see the great deal of attention that the round jet has received in the last century. There remain some significant outstanding questions. Starting with the route to self similarity. Is there a universal route? How do jets attain self-similarity? It is worthwhile to examine the physical route as the jet develops from its origin to its far-field self-similar state. The striking difference between sub- and super-transitional jet flows observed by Dimotakis [59] corresponds to differences in the structures (as found by Liepmann and Gharib [82] in the near field), and most likely to the velocity statistics and scales (as found by Fellouah and Pollard [83]). What are the changes in the velocity fields (mean and fluctuating) in the near field as the jet flow evolves through the mixing transition? And, how do these changes cause the phenomena observed qualitatively and in the passive scalar? Moreover, if the mixing transition is reflected in the development of the velocity fields (mean and fluctuating), how is the route to self-similarity affected?

Another question that can be raised from this review is: Are the virtual origin and jet half-width real? In Uddin and Pollard [43], the physical validity of the virtual origin, x_0 and the jet half-width length scale $r_{1/2}$ are questioned in light of results from LES of axisymmetric co-flowing jets.

Finally, the continued development of particle image velocimetry, and more recently the advent of both tomographic and time resolved PIV are an exciting addition to the arsenal of the experimentalist; turbulence research has benefited enormously by the continuing

development of computational tools and hardware. In 2011, the fidelity of data obtained from these two approaches is becoming similar. The investigation of the structure of turbulence in a jet will depend increasingly on direct numerical simulations and pushed to ever higher Reynolds numbers. We noted the paucity of data in the intermediate fields of jets, which we believe to be where all the exciting interactions occur. But, understandably, the canonical free round jet has limited utility in real-life applications and so detailed investigations will likely focus on jets under the influence of external disturbances, and on evolution of jets that issue from geometrically altered orifice shapes, all under a wide range in Reynolds number.

Very briefly ... What is known:

- Coherent structures establish the evolution of the flow.
- The study of structures, energy, and modes gives us the best nearly-objective view of the flow.
- Initial conditions (inlet conditions) are carried through to the far field.
- There probably exists a mixing transition (between low and high Reynolds number, and between the near and far fields).
- There is a modest selection of methods that allow limited observation of the flow.

And, what is not yet known:

- The precise nature of the interactions (beyond energy transfer) among coherent structures.
- The mixing transition.
- How to interact with coherent structures.

Acknowledgments

This work was supported financially by the Natural Sciences and Engineering Research Council of Canada through its Discovery and Equipment Grants programmes. AP also acknowledges the Queens Research Chair Programme.

References

[1] Davidson PA. Turbulence: an introduction for scientists and engineers. Oxford University Press; 2005.
[2] Fiedler HE. Control of free turbulent shear flows. In: el Hak MG, Pollard A, Bonnet JP, editors. Flow control: fundamentals and practices. Springer-Verlag; 1998. p. 335–429.
[3] Kolmogorov AN. The local structure of turbulence in an incompressible viscous fluid at very high Reynolds' numbers. Doklady Akademii Nauk SSSR 1941;30:299–303.
[4] George WK. The self-preservation of turbulent flows and its relation to initial conditions and coherent structures. In: Arndt REA, George WK, editors, Advances in turbulence, Hemisphere, New York; 1989. p. 39–73.
[5] Johansson PBV, George WK, Gourlay MJ. Equilibrium similarity, effects of initial conditions and local Reynolds number on the axisymmetric wake. Physics of Fluids 2003;15:603.
[6] Sreenivasan KR, Antonia RA. The phenomenology of small-scale turbulence. Annual Review of Fluid Mechanics 1997;29(1):435–72.
[7] Samimy M, Kim J-H, Kastner J, Adamovich I, Utkin Y. Active control of high-speed and high-Reynolds-number jets using plasma actuators. Journal of Fluid Mechanics 2007;578:305–30.
[8] Mitsuishi A, Fukagata K, Kasagi N. Near-field development of large-scale vortical structures in a controlled confined coaxial jet. Journal of Turbulence 2007;8(23):1–27.
[9] Wei M, Freund JB. A noise-controlled free shear flow. Journal of Fluid Mechanics 2005;546:123–52.
[10] Hall JW, Hall AM, Pinier JT, Glauser MN. Cross-spectral analysis of the pressure in a Mach 0.85 turbulent jet. AIAA Journal 2009;47:54–9.
[11] Richardson LF. Weather prediction by numerical process. Cambridge University Press; 1922.
[12] Abramovich GN. The theory of turbulent jets. Cambridge, MA: MIT Press, Massachusetts Institute of Technology; 1963.
[13] Ruden P. Turbulente aurbreitungsvorgange im freistrahl. Naturwissenschaften 1933;21(21–23):375–8.
[14] Kuethe AM. Investigations of the turbulent mixing regions formed by jets. Journal of Applied Mechanics 1935;2(3):A87–95.
[15] Dowling DR, Dimotakis PE. Similarity of the concentration field of gas-phase turbulent jets. Journal of Fluid Mechanics 1990;218:109–41.
[16] Squire HB, Trouncer J. Round jets in a general stream. Reports and memoranda no. 1974, Aeronautical Research Committee, London; 1944.
[17] Wygnanski I, Fiedler HE. Some measurements in the self-preserving jet. Journal of Fluid Mechanics 1969;38:577–612.
[18] Tollmien W. Berechnung turbulenter ausbreitungsvorgänge. Zeitschrift fur Angewandte Mathematic und Mechanik 1945;6(468). (see also, NACA TN 1085. Available at: 〈http://ntrs.nasa.gov/〉).
[19] Ricou FP, Spalding DB. Measurements of entrainment by axisymmetrical turbulent jets. Journal of Fluid Mechanics 1961;11:21–32.
[20] Kuethe AM. Investigations of turbulent mixing regions, PhD thesis. California Institute of Technology, Pasadena, CA; 1933.
[21] Corrsin S. Investigation of flow in an axially symmetrical heated jet of air. Advance confidential report 3L23, National Advisory Committee for Aeronautics; 1943.
[22] Corrsin S, Uberoi MS. Further experiments on the flow and heat transfer in a heated turbulent air jet. NACA technical report No. 998.
[23] King LV. On the convection of heat from small cylinders in a stream of fluid: determination of the convection constants of small platinum wires with applications to hot-wire anemometry. Philosophical Transactions of the Royal Society of London. Series A, Containing Papers of a Mathematical or Physical Character 1914;214:373–432.
[24] Wattendorf FL, Kuethe AM. Investigations of turbulent flow by means of the hot-wire anemometer. Physics 1934;5(6):153–64.
[25] Liepmann HW, Laufer J. Investigations of free turbulent mixing. Technical note 1257, National Advisory Committee for Aeronautics; 1947.
[26] Pai SI. Fluid dynamics of jets. Princeton, NJ: Van Nostrand, MacMillan; 1954.
[27] Schetz JA. Injection and mixing in turbulent flow. New York, NY: American Institute of Aeronautics and Astronautics; 1980.
[28] Laurence JC. Intensity, scale, and spectra of turbulence in mixing region of free subsonic jet. NACA report 1292, National Advisory Committee for Aeronautics; 1956.
[29] Huppert HE. George Keith Batchelor: 8 March 1920–30 March 2000 founding editor of Journal of Fluid Mechanics 1956. Journal of Fluid Mechanics 2000;421:1–142155.
[30] Zhang S, Schneider SP. Quantitative molecular-mixing measurements in a round jet with tabs. Physics of Fluids 1995;7:1063.
[31] Waterman S, Holme T, McIlwain S, Pollard A. Investigation of various structure identification methods and the effects of tabs on the near field of round jets. ASME Conference Proceedings 2002, 36169; 2002. p. 1135–42.
[32] Suzuki H, Kasagi N, Suzuki Y, Shima H. Manipulation of a round jet with electromagnetic flap actuators. In: Twelfth IEEE international conference on micro electro mechanical systems. Orlando, FL; 1999. p. 534–40.
[33] Davies POAL, Fisher MJ, Barrat MJ. The characteristics of the turbulence in the mixing region of a round jet. Journal of Fluid Mechanics 1963;15:337–67.
[34] Sami S, Carmody T, Rouse H. Jet diffusion in the region of flow establishment. Journal of Fluid Mechanics 1967;27:231–52.
[35] Rodi W. A new method of analysing hot-wire signals in highly turbulent flow and its evaluation in a round jet. DISA Information 1975; 17.
[36] Seif AA. Higher order closure model for turbulent jets. PhD thesis. SUNY Buffalo; 1981.
[37] Nathan GJ, Mi J, Alwahabi ZT, Newbold GJR, Nobes DS. Impacts of a jet's exit flow pattern on mixing and combustion performance. Progress in Energy and Combustion Science 2006;32(5–6):496–538.
[38] Hinze JO. Turbulence. New York: McGraw-Hill; 1975.
[39] George WK, Davidson L. Role of initial conditions in establishing asymptotic behaviour. AIAA Journal 2004;42(3):438–46.
[40] Richards CD, Pitts WM. Global density effects on the self-preservation behaviour of turbulent free jets. Journal of Fluid Mechanics 1993;254:417–35.
[41] Mi J, Nobes DS, Nathan GJ. Influence of jet exit conditions on the passive scalar field of an axisymmetric free jet. Journal of Fluid Mechanics 2001;432:91–125.
[42] Quinn WR. Upstream nozzle shaping effects on near field flow in round turbulent free jets. European Journal of Mechanics/B Fluids 2006;25:279–301.
[43] Uddin M, Pollard A. Self-similarity of coflowing jets: the virtual origin. Physics of Fluids 2007;19:068103.
[44] Verzicco R, Orlandi P. Mixedness in the formation of a vortex ring. Physics of Fluids 1995;7:1513.
[45] Romano GP. The effect of boundary conditions by the side of the nozzle of a low Reynolds number jet. Experiments in Fluids 2002;33(2):323–33.
[46] Yoda M, Hesselink L, Mungal MG. The evolution and nature of large-scale structures in the turbulent jet. Physics of Fluids A: Fluid Dynamics 1992;4:803–11.
[47] Yoda M, Hesselink L, Mungal MG. Instantaneous three-dimensional concentration measurements in the self-similar region of a round high-Schmidt-number jet. Journal of Fluid Mechanics 1994;279:313–50.
[48] Hrycak P, Jachna S, Lee DT. A study of characteristics of developing, incompressible, axi-symmetric jets. Letters Heat Mass Transfer 1974;1:63–71.
[49] Panchapakesan NR, Lumley JL. Turbulence measurements in axisymmetric jets of air and helium. Part 1. Air jet. Journal of Fluid Mechanics 1993;246:197.

[50] Schlichting H. Boundary layer theory. 7th ed. New York: McGraw-Hill; 1979.
[51] Hussein HJ, Capp SP, George WK. Velocity measurements in a high-Reynolds-number, momentum-conserving, axisymmetric, turbulent jet. Journal of Fluid Mechanics 1994;258:31–75.
[52] Xu G, Antonia RA. Effect of different initial conditions on a turbulent round free jet. Experiments in Fluids 2002;33:677–83. URL 〈http://www.springerlink.com/index/QQAA11T3V5122D5H.pdf〉.
[53] Citriniti JH, George WK. Reconstruction of the global velocity field in the axisymmetric mixing layer utilizing the proper orthogonal decomposition. Journal of Fluid Mechanics 2000;418:137–66.
[54] McIlwain S, Pollard A. Large eddy simulation of the effects of mild swirl on the near field of a round free jet. Physics of Fluids 2002;14:653.
[55] Capp SP. Experimental investigation of the turbulent axisymmetric jet. PhD thesis. SUNY Buffalo; 1983.
[56] George WK, Capp SP, Seif AA, Baker CB, Taulbee DB. A study of the turbulent axisymmetric jet. Journal of King Saud University (Engineering Science) 1988;14:85–93.
[57] Iqbal MO, Thomas FO. Coherent structure in a turbulent jet via a vector implementation of the proper orthogonal decomposition. Journal of Fluid Mechanics 2007;571:281–326.
[58] Capp SP, Hussein HJ, George WK. Velocity measurements in a high-Reynolds-number, momentum-conserving, axisymmetric, turbulent jet. Technical report 123, SUNY Buffalo, Turbulence Research Laboratory; 1990.
[59] Dimotakis PE. The mixing transition in turbulent flows. Journal of Fluid Mechanics 2000;409:69–98.
[60] Donald MB, Singer H. Entrainment in turbulent jets. Transactions of the Institute of Chemical Engineering 1959;37:255–67.
[61] Hill BJ. Measurement of local entrainment rate in the initial region of axisymmetric turbulent air jets. Journal of Fluid Mechanics 1972;51:773–9.
[62] Bradshaw P. The effect of initial conditions on the development of a free shear layer. Journal of Journal of Fluid Mechanics 1966;26:225–36.
[63] Lai JCS. The preferred mode of a tube jet. International Journal of Heat and Fluid Flow 1991;12(3):284–6.
[64] Crow SC, Champagne FH. Orderly structure in jet turbulence. Journal of Fluid Mechanics 1971;48(3):547–91.
[65] Ko NWM, Davies POAL. The near field within the potential cone of subsonic cold jets. Journal of Fluid Mechanics 1971;50:49–78.
[66] Ko NWM, Kwan ASH. The initial region of subsonic coaxial jets. Journal of Fluid Mechanics 1976;73:305–32.
[67] Boersma BJ, Brethouwer G, Nieuwstadt FTM. A numerical investigation on the effect of the inflow conditions on the self-similar region of a round jet. Physics of Fluids 1998;10:899.
[68] Martin JE, Meiburg E, Lasheras JC. Three-dimensional evolution of axisymmetric jets: a comparison between computations and experiments. In: Kozlov VV, Dovgal AV, editors. Separated flows and jets. Berlin: Springer-Verlag; 1991.
[69] Olsson M, Fuchs L. Large eddy simulation of the proximal region of a spatially developing circular jet. Physics of Fluids 1996;8:2125.
[70] Ferdman E, Otugen MV, Kim S. Effect of initial velocity profile on the development of the round jet. Journal of Propulsion and Power 2000;16:676–86.
[71] Romano GP, Antonia RA. Longitudinal and transverse structure functions in a turbulent round jet: effect of initial conditions and Reynolds number. Journal of Fluid Mechanics 2001;436:231–48.
[72] Antonia RA, Zhao Q. Effect of initial conditions on a circular jet. Experiments in Fluids 2001;31(3):319–23.
[73] Burattini P, Antonia RA, Rajagopalan S, Stephens M. Effect of initial conditions on the near-field development of a round jet. Experiments in Fluids 2004;37(1):56–64.
[74] Burattini P, Djenidi L. Velocity and passive scalar characteristics in a round jet with grids at the nozzle exit. Flow, Turbulence and Combustion 2004;72(2):199–218.
[75] Burattini P, Antonia RA, Danaila L. Similarity in the far field of a turbulent round jet. Physics of Fluids 2005;17:025101.
[76] Rajagopalan S, Antonia RA. Turbulence and drag control in jet and wake flows. Sadhana 2007;32(1):133–44.
[77] Carazzo G, Kaminski E, Tait S. The route to self-similarity in turbulent jets and plumes. Journal of Fluid Mechanics 2006;547:137–48.
[78] Nickels TB, Perry AE. An experimental and theoretical study of the turbulent co-flowing jet. Journal of Fluid Mechanics 1996;309:157–82.
[79] Townsend AA. The structure of turbulent shear flow. Cambridge, UK: Cambridge University Press; 1976.
[80] Dimotakis PE, Miake-Lye RC, Papantoniou DA. Structure and dynamics of round turbulent jets. Physics of Fluids 1983;26:3185.
[81] Miller PL, Dimotakis PE. Reynolds number dependence of scalar fluctuations in a high Schmidt number turbulent jet. Physics of Fluids A 1991;3(5):1156–63.
[82] Liepmann D, Gharib M. The role of streamwise vorticity in the near-field entrainment of round jets. Journal of Fluid Mechanics 1992;245:643.
[83] Fellouah H, Pollard A. The velocity spectra and turbulence length scale distributions in the near to intermediate regions of a round free turbulent jet. Physics of Fluids 2009;21:115101.
[84] Fellouah H, Ball CG, Pollard A. Reynolds number effects within the development region of a turbulent round free jet. International Journal of Heat and Mass Transfer 2009;52(17–18):3943–54.
[85] Ewing D, Frohnapfel B, George WK, Pedersen JM, Westerweel J. Two-point similarity in the round jet. Journal of Fluid Mechanics 2007;577:309–30.
[86] Kolmogorov AN. Dissipation of energy in the locally isotropic turbulence. Doklady Akademii Nauk SSSR 1941;32(4):16–8.
[87] Saddoughi SG, Veeravalli SV. Local isotropy in turbulent boundary layers at high Reynolds number. Journal of Fluid Mechanics 1994;268:333–72.
[88] Zhou Y, Robey HF, Buckingham AC. Onset of turbulence in accelerated high-Reynolds-number flow. Physical Review E 2003;67(5):56305.
[89] Antonia RA, Satyaprakash BR, Hussain AKMF. Measurements of dissipation rate and some other characteristics of turbulent plane and circular jets. Physics of Fluids 1980;23:695.
[90] Becker HA, Massaro TA. Vortex evolution in a round jet. Journal of Fluid Mechanics 1968;31:435–48.
[91] List EJ. Turbulent jets and plumes. Annual Review of Fluid Mechanics 1982;14(1):189–212.
[92] Wehrmann O, Wille R. Beitrag zur phänomenologie des laminar-turbulenten ubergange im freistrahl bei kleinen reynoldszahlen. In: Görtler H, editor. Boundary layer research IUTAM symposium; 1957. p. 387–403.
[93] Freymuth P. On transition in a separated laminar boundary layer. Journal of Fluid Mechanics 1966;25:683–704.
[94] Schneider PEM. Sekundärwirbelbildung dei ringwirbeln und in freistrahlen. Zeitschrift für Flugwissenschaften und Weltraumforschung 1980;4(5):307–18.
[95] Yule AJ. Large-scale structure in the mixing layer of a round jet. Journal of Fluid Mechanics 1978;89:413–32.
[96] Brown GB. On vortex motion in gaseous jets and the origin of their sensitivity to sound. Proceedings of the Physical Society 1935;47:703–32.
[97] Plaschko P. Helical instabilities of slowly divergent jets. Journal of Fluid Mechanics 1979;92:209–15.
[98] Freeman RW, Tavlarides LL. Observations of the instabilities of a round jet and the effect of concurrent flow. Physics of Fluids 1979;22(4):782–3.
[99] Robinson SK. Coherent motions in the turbulent boundary layer. Annual Review of Fluid Mechanics 1991;23(1):601–39.
[100] Fiedler HE. Coherent structures in turbulent flows. Progress in Aerospace Sciences 1988;25(3):231–69.
[101] Mungal MG, Hollingsworth DK. Organized motion in a very high Reynolds number jet. Physics of Fluids A: Fluid Dynamics 1989;1:1615.
[102] Hussain AKMF. Coherent structures and turbulence. Journal of Fluid Mechanics 1986;173:303–56.
[103] Dyke MV. An album of fluid motion. Stanford, CA: Parabolic Press; 1982.
[104] Ho CM, Huerre P. Perturbed free shear layers. Annual Review of Fluid Mechanics 1984;16:365–424.
[105] Huerre P, Monkewitz PA. Absolute and convective instabilities in free shear flows. Journal of Fluid Mechanics 1985;159:151–68.
[106] Huerre P, Monkewitz PA. Local and global instabilities in spatially developing flows. Annual Review of Fluid Mechanics 1990;22:473–537.
[107] Hussain AKMF, Clark AR. On the coherent structure of the axisymmetric mixing layer: a flow-visualiszation study. Journal of Fluid Mechanics 1981;104:263–94.
[108] Hama FR. Streaklines in a perturbed shear flow. Physics of Fluids 1962;5:644.
[109] Glauser MN. Coherent structures in the axisymmetric turbulent jet mixing layer. PhD thesis. SUNY Buffalo; 1987.
[110] Glauser MN, George WK. Orthogonal decomposition of the axisymmetric jet mixing layer including azimuthal dependence. In: Advances in turbulence: Proceedings of the first European turbulence conference; 1987. p. 357–66.
[111] Glauser MN, Leib SJ, George WK. Coherent structures in the axisymmetric turbulent jet mixing layer. Turbulent Shear Flows 1987;5:134–45.
[112] Tso J, Hussain F. Organized motions in a fully developed turbulent axisymmetric jet. Journal of Fluid Mechanics 1989;203:425–48.
[113] Kirby M, Boris J, Sirovich L. An eigenfunction analysis of axisymmetric jet flow. Journal of Computational Physics 1990;90(1):98–122.
[114] Dahm WJA, Dimotakis PE. Mixing at large Schmidt number in the self-similar far field of turbulent jets. Journal of Fluid Mechanics 1990;217:299–330.
[115] Agrawal A, Prasad AK. Organizational modes of large-scale vortices in an axisymmetric turbulent jet. Flow, Turbulence and Combustion 2002;68(4):359–77.
[116] Cenedese A, Doglia G, Romano GP, Michele GD, Tanzini G. LDA and PIV velocity measurements in free jets. Experimental Thermal and Fluid Science 1994;9(2):125–34.
[117] Paschereit CO, Oster D, Long TA, Fiedler HE, Wygnanski I. Flow visualization of interactions among large coherent structures in an axisymmetric jet. Experiments in Fluids 1992;12(3):189–99.
[118] Weisgraber TH, Liepmann D. Turbulent structure during transition to self-similarity in a round jet. Experiments in Fluids 1998;24:210–24. URL 〈http://www.springerlink.com/index/A5Y3T7C5VQKXW7AR.pdf〉.
[119] Drobniak S, Elsner JW, El-Kassem E-SA. The relationship between coherent structures and heat transfer processes in the initial region of a round jet. Experiments in Fluids 1998;24(3):225–37.
[120] Lavoie P, Pollard A. Uncertainty analysis of four-sensor hot-wires and their data-reduction schemes used in the near field of a turbulent jet. Experiments in Fluids 2003;34(3):358–70.
[121] Sullivan P, Pollard A. Coherent structure identification from the analysis of hot-wire data. Measurement Science and Technology 1996;7:1498.
[122] Bonnet JP, Delville J, Glauser MN, Antonia RA, Bisset DK, Cole DR, Fiedler HE, Garem JH, Hilberg D, Jeong J. Collaborative testing of eddy structure identification methods in free turbulent shear flows. Experiments in Fluids 1998;25(3):197–225.

[123] Glauser MN, George WK. Application of multipoint measurements for flow characterization. Experimental Thermal and Fluid Science 1992;5(5): 617–32.
[124] Arndt REA, Long DF, Glauser MN. The proper orthogonal decomposition of pressure fluctuations surrounding a turbulent jet. Journal of Fluid Mechanics 1997;340:1–33.
[125] Glauser M. October 2010. URL 〈http://www.ecs.syr.edu/faculty/glauser/〉.
[126] Ganapathisubramani B, Longmire EK, Marusic I. Investigation of three dimensionality in the near field of a round jet using stereo PIV. Journal of Turbulence 2002;3(1):1–12.
[127] Hunt JCR, Wray AA, Moin P. Eddies, stream and convergence zones in turbulent flows. In: Proceedings of the 1988 summer programme, Center for Turbulence Research, Stanford University; 1988. p. 193–208.
[128] Sheridan E, Pollard A. Interrogation of the LES generated flow field of a round jet using a variety of structure eduction approaches, in preparation.
[129] Agrawal A, Prasad AK. Properties of vortices in the self-similar turbulent jet. Experiments in Fluids 2002;33(4):565–77.
[130] Agrawal A, Prasad AK. Measurements within vortex cores in a turbulent jet. Journal of Fluids Engineering 2003;125:561.
[131] Agrawal A. Analysis of vortex cores in turbulent flows. Journal of Turbulence 2010;11(42):359–77.
[132] Jung D, Gamard S, George WK. Downstream evolution of the most energetic modes in a turbulent axisymmetric jet at high Reynolds number. Part 1. The near-field region. Journal of Fluid Mechanics 2004;514:173–204.
[133] Gamard S, Jung D, George WK. Downstream evolution of the most energetic modes in a turbulent axisymmetric jet at high Reynolds number. Part 2. The far-field region. Journal of Fluid Mechanics 2004;514:205–30.
[134] Gamard S, George WK, Jung D, Woodward S. Application of a "slice" proper orthogonal decomposition to the far field of an axisymmetric turbulent jet. Physics of Fluids 2002;14:2515.
[135] Suto H, Matsubara K, Kobayashi M, Kaneko Y. Large eddy simulation of flow and scalar transport in a round jet. Heat Transfer: Asian Research 2004;33(3): 175–88.
[136] Suto H, Matsubara K, Kobayashi M, Watanabe H, Matsudaira Y. Coherent structures in a fully developed stage of a non-isothermal round jet. Heat Transfer: Asian Research 2004;33(5):342–56.
[137] Matsuda T, Sakakibara J. On the vortical structure in a round jet. Physics of Fluids 2005;17:025106.
[138] Kwon SJ, Seo IW. Reynolds number effects on the behavior of a non-buoyant round jet. Experiments in Fluids 2005;38(6):801–12.
[139] Bogey C, Bailly C. Large eddy simulations of transitional round jets: influence of the Reynolds number on flow development and energy dissipation. Physics of Fluids 2006;18:065101.
[140] Shinneeb A-M, Balachandar R, Bugg JD. Analysis of coherent structures in the far-field region of an axisymmetric free jet identified using particle image velocimetry and proper orthogonal decomposition. Journal of Fluids Engineering 2008;130:1–9. URL 〈http://link.aip.org/link/?JFEGA4/130/011202/1〉.
[141] Shinneeb A-M, Bugg JD, Balachandar R. Quantitative molecular-mixing measurements in a round jet with tabs. Journal of Turbulence 2008;9(19): 1–20.
[142] Jeong J, Hussain F. On the identification of a vortex. Journal of Fluid Mechanics 1995;285:69–94.
[143] Russ S, Strykowski PJ. Turbulent structure and entrainment in heated jets: the effect of initial conditions. Physics of Fluids A: Fluid Dynamics 1993;5:3216.
[144] Priestley CHB, Ball FK. Continuous convection from an isolated source of heat. Quarterly Journal of the Royal Meteorological Society 1955;81: 144–57.
[145] Ball CG, Pollard A. A review of experimental and computational studies of flow from the round jet. Computational and experimental fluid dynamics laboratory. CEFDL 2007/01, Queen's University; 2007.
[146] Boguslawski L, Popiel CO. Flow structure of the free round turbulent jet in the initial region. Journal of Fluid Mechanics 1979;90:531–9.
[147] Quinn WR, Militzer J. Effects of nonparallel exit flow on round turbulent free jets. International Journal of Heat and Fluid Flow 1989;10(2):139–45.
[148] Abdel-Rahman AA, Chakroun W, Al-Fahed SF. Lda measurements in the turbulent round jet. Mechanics Research Communications 1997;24(3): 277–88.
[149] Chevray R, Tutu NK. Intermittency and preferential transport of heat in a round jet. Journal of Fluid Mechanics 1978;88(1):133–60.